

MUTAGENESIS AND FUNCTIONAL ANALYSIS OF *dveli*

**MUTAGENESIS AND FUNCTIONAL ANALYSIS OF *dveli*, THE *DROSOPHILA*
ORTHOLOG OF *C. ELEGANS Lin-7***

by

YING-HSU HUANG, B.Sc.

A Thesis
Submitted to the School of Graduate Studies
in Partial fulfillment of the Requirements
for the Degree
Master of Science

McMaster University

© Copyright by Ying-Hsu Huang, March 2004

McMASTER UNIVERSITY LIBRARY

MASTER OF SCIENCE (2004)
(Biology)

McMaster University
Hamilton, Ontario

TITLE: Mutagenesis and functional analysis of *dveli*, the *Drosophila* ortholog of
C. elegans lin-7

AUTHOR: Ying-Hsu Huang, B.Sc., Concordia University

SUPERVISOR: J. Roger Jacobs, Ph.D., Professor, McMaster University

NUMBER OF PAGES: xi, 121

ABSTRACT

Proper assembly and localization of receptors and the associated signal transduction protein complex is important for normal cell function. Scaffolding proteins have been implicated in organizing the assembly of protein complex and localization of receptors. PDZ domain containing proteins are one major type of scaffolding protein. One well characterized system is the *C. elegans* LIN-2/LIN-7/LIN-10 PDZ protein complex. In *C. elegans*, this protein complex acts as a scaffold for the proper localization of LET-23, the ortholog of EGFR, to the epithelial basolateral membrane.

The *Drosophila* orthologs, *cmg*, *dveli* and *dmint/dX11L*, have been identified. The sequence homologies and expression patterns suggest that these genes may have similar functions as their mammalian orthologs. The possible functions include cell-cell junction formation, receptor localization, ion channel localization and neurotransmitter vesicle trafficking.

The main objectives of this thesis work are the mutagenesis and functional analysis of *dveli*. Potential mutants were generated by P element insertional mutagenesis, however, further analysis is required to identify the affected genes. A systemic RNAi experiment was performed. The delivery mechanism used was the RNAi soaking technique adapted from Dr. Davis's laboratory protocol. Primary results from RNAi experiments show that loss of *dveli* function results in a reduction in larval locomotion speed. This slower locomotion phenotype along with the post-synaptic expression of dVELI at larval neuromuscular junction suggest a synaptic role of dVELI, perhaps aiding in synapse formation or proper localization of neurotransmitter receptors.

ACKNOWLEDGEMENTS

To my supervisor Dr. Roger Jacobs, thank you for all advises and guidance of this project. It has been a very rewarding research experience for me, and for this I am forever grateful. To my committee members Dr. Ana Campos and Dr. Colin Nurse, thank you for taking the time to examine this thesis and for all the suggestions for improving this thesis.

To members of Jacobs lab, thank you all very much. To Oliver Krupke and Allison MacMullin, thank you for all the advises and suggestions to help with my experiments. To Dr. Miheala Georgescu, Kelly Teal, Leena Patel, and Katie Moyer, thank you for your support, laughter and friendship. To Dr. Chun mei Wang and Dr. Firoz Mian, thank you as well for your help. To Maria Papaconstantinou and Nadia Scantlebury from Campos lab, thank you as well for the technical support and suggestions.

Finally, to my family and friends back home, thank you all for your encouragement and support that allowed me to continue this study. I couldn't do it without you.

TABLE OF CONTENTS

PAGE

Title page	i
Descriptive Note	ii
Abstract	iii
Acknowledgements	iv
Table of Contents	v
List of Figures	viii
Abbreviations	ix
Contributions	xi
CHAPTER 1: INTRODUCTION	1
1.1 PDZ domain and PDZ domain containing proteins	1
1.2 PDZ proteins and epithelial cell polarity	4
1.3 PDZ proteins at synaptic junction	9
1.4 The LIN-2/LIN-7/LIN-10 PDZ protein complex	12
1.5 Mammalian homologs of LIN-2/LIN-7/LIN-10	14
1.6 <i>Drosophila</i> homologs of LIN-2, LIN-7, and LIN-10	18
1.7 <i>Drosophila</i> as a model organism to study function of dVELI	23
CHAPTER 2: MATERIALS AND METHODS	25
2.1 <i>Drosophila melanogaster</i> Strains	25
2.2 Embryos, larva and adult fly collection	25
2.3 P element mutagenesis	26
2.4 Confirmation of original P element insertion by PCR	27
2.5 Preparation of genomic DNA for PCR screen	28
2.6 UAS-GAL4 misexpression	29
2.7 Generation of <i>dveli</i> His fusion construct	29
2.8 Expression of dVELI HIS fusion protein	30
2.9 Purification of dVELI HIS fusion protein	30
2.10 Preparation of dialysis tubing	31
2.11 Affinity purification of anti-dVELI antibody	32
2.12 Immunostaining of larval central nervous system	33
2.13 Preparation of crude protein from <i>Drosophila</i> tissue	33
2.14 Protein concentration determination	34
2.15 Western Blot analysis	35
2.16 Preparation of double stranded RNA template constructs	36
2.17 <i>in vitro</i> transcription of double stranded RNA	37
2.18 RNAi soaking technique	38

2.19	Quantitative beta-galactosidase activity assay	38
2.20	Larval locomotion behavior assay recording and measurement	39
CHAPTER 3: RESULTS		40
3.1	P element insertional mutagenesis	41
	-Confirmation of original P element insertion	42
	-Genetics of P element mobilization	49
	-Deficiency screen	50
	-PCR screen	55
3.2	Purification of anti-dVELI antibody	60
	-Analysis of the purified antibody	60
3.3	Misexpression of dVELI using UAS-GAL4 expression system	65
	-Effects of dVELI misexpression-viability tests	66
	-Western blot analysis for confirmation of protein expression	71
3.4	RNA interference	74
	-Locomotion behavior effects upon RNA interference	74
	-Immunostaining of larval CNS to confirm silencing of gene expression by RNAi	75
CHAPTER 4: DISCUSSION		80
4.1	Generation and analysis of potential <i>dveli</i> mutants	80
4.2	Analysis of dVELI antibody shows the specificity of this antibody	84
4.3	Misexpression of dVELI by the UAS-GAL4 system fail to show significant effects on viability, which may due to invalid UAS constructs	85
4.4	RNA interference tests indicate that <i>dveli</i> is involved in locomotion behavior	87
4.5	Potential formation of CMG/dVELI/dX11L complex and its function	90
4.6	Direction of future research	93
REFERENCES		95
APPENDICES		103
Appendix 1	Adult fly grooming behavior assay	104

Appendix 2	Time required for adult flies to recover from CO ₂ treatment	107
Appendix 3	Genetic scheme for mapping the chromosomal location of UAS-lin7s	109
Appendix 4	pET29b+ multiple cloning sites	111
Appendix 5	LITMUS 28i multiple cloning sites	113
Appendix 6	Locomotion behavior test of dsRNA treated larvae	115
Appendix 7	beta-galactosidase activity assay for ds lacZ efficiency	117
Appendix 8	Deficiency screen results	120

LIST OF FIGURES		PAGE
Figure 1	Proteins interact with CASK, Velis and Mints	19
Figure 2	Schematic of the PCR method for confirming P element insertion	43
Figure 3	PCR result	45
Figure 4	Sequence alignment	47
Figure 5	Genetics of P element mobilization	51
Figure 6	Genetics scheme of deficiency screen	53
Figure 7	Schematic of PCR screen	57
Table 1	PCR screen result	59
Figure 8	Western blot analysis of CS-P adult fly whole protein	61
Figure 9	Immunostaining of CS-P larval CNS	63
Figure 10	Embryo viability	67
Figure 11	Larval viability	69
Figure 12	Western blot analysis for confirmation of d VELI expression of the UAS-lin7 constructs	72
Figure 13	Locomotion behavior test result	76
Figure 14	Immunostaining of larval CNS showing RNAi effect on gene expression	78

LIST OF ABBREVIATIONS

APP	Amyloid- β precursor protein
BDGP	Berkeley <i>Drosophila</i> Genome Project
CAM	cell adhesion molecules
CASK	Calcium/calmodulin dependent serine kinase
CMG	Camguk
CNBr	Cyanogen bromide
CNS	Central Nervous system
CS-P	Canton S-P-element free
DAB	3,3'-Diaminobenzidine tetrahydrochloride
DER	<i>Drosophila</i> EGFR
DLG	Discs large
DVELI	<i>Drosophila</i> Veli
EGFR	Epidermal growth factor receptor
FasII	Fasciclin II
GABA	Gamma-aminobutyric acid
GAL4	Galactosidase transgene with 4 binding sites
GK	Guanylate kinase-like domain
GuK	Guanylate kinase
GUKH	Guk holder
HRP	Horseradish peroxidase
IPTG	isopropylthio-beta-D-galactoside
L27	LIN-2/LIN-7 heterodimerization domain
Lgl	Lethal giant larvae
LRR	Leucine-rich repeats
MAGUK	Membrane associated guanylate kinase
Mint	Munc 18-1 interaction
MRE	MAGUK recruitment
MZ	Marginal zone
NMDA	N-methyl-D-aspartate type glutamate receptor
NMJ	Neuromuscular junction
PAGE	Polyacrylamide gel electrophoresis
PALS	Proteins associated with LIN-7
PATJ	Pals1-associated tight junction
PBS	Phosphate buffered saline
PBT	PBS with Triton
PCR	Polymerase chain reaction
PDZ	Post-synaptic density-95/Discs large A/Zona occludens-1
PSD-95	Post synaptic density-95
PTB	Phosphotyrosine binding
RTK	Receptor tyrosine kinase
SAPs	Synapse associated proteins
SDS	Sodium dodecyl sulphate

SH3	Src Homology 3
SJ	Septate junction
TGF	Transforming growth factor
TJ	Tight junction
UAS	Upstream activating sequence
VELI	Vertebrate LIN-7
ZA	Zonula adherens
ZO-1	Zona occludens-1

Contributions

Dr. Chun mei Wang generated the LITMUS 28i *dveli* construct for double-stranded *dveli* RNA synthesis. Nadia Scantlebury, Dr. Campos lab, McMaster University, did statistical analysis of locomotion behavior tests.

Chapter 1

Introduction

Protein complex formation and proper localization of proteins are very important for maintaining normal cellular function. For example, cell polarity establishment and maintenance is crucial for proper development and function of organisms. Without proper localization and assembly of proteins at the plasma membrane, communication errors between cells would occur and lead to cellular function disruption. One major type of protein that acts as a scaffold for protein complex assembly is the PDZ domain containing proteins. Scaffolding protein complexes containing PDZ proteins have been shown to function in synapse assembly, signal transduction, establishment of cell polarity and protein sorting such as the proper localization of LET-23 by the LIN-2/LIN-7/LIN-10 PDZ protein complex in *C. elegans* (Simske et al, 1996). The *Drosophila* homolog of LIN-7, dVELI, contains a PDZ domain and is hypothesized to function in proper localization of receptors as its *C. elegans* homolog. The main focus of this thesis is to study the function of this PDZ domain containing protein, dVELI.

1.1 PDZ domain and PDZ domain containing proteins

The PDZ domain is a protein domain that contains about 90 amino acids. It was first identified as a common structure in the postsynaptic protein PSD-95/SAP90, the *Drosophila* tumor suppresser protein Discs-large (Dlg), and the tight junction protein Zona occludens 1 (ZO-1), hence the name PDZ (Sheng and Sala, 2001). PDZ domains are found in a lot of proteins among diverse organisms from bacteria, yeast, plant,

nematode, fruitfly to mammals. Based on an analysis of the *Drosophila* genome by Schultz et al, there are at least 133 PDZ domains present in 86 proteins (Schultz et al, 2000). A characteristic of PDZ domain-containing proteins is that they usually contain multiple PDZ domains. It is speculated that the multiple copies of the PDZ domain can cooperate to enhance binding to target peptides (Hung and Sheng, 2002). For example, the scaffolding protein syntenin contains two PDZ domains. The second PDZ domain binds to the C-terminal peptides of syndecan, neuexin, and ephrin-B1. However, this interaction only occurs when both of the PDZ domains are present in syntenin (Grootjans et al, 2000).

The most common interaction between the PDZ domain and other proteins is the binding of the PDZ domain to the extreme C-terminal peptide of its binding partner. This interaction was first found in the interaction between the first and second PDZ domain of PSD-95 and the C-terminal peptides of Shaker-type K^+ channels and NMDA receptor NR2 subunits (Kim et al, 1995; Kornau et al, 1995). Crystallography studies revealed the structures of PDZ domains and the structural basis of PDZ binding. The common structure of PDZ domain consists of six β strands (βA - βF) and two α helices (αA and αB) (Doyle et al, 1996; Morais Cabral et al, 1996). The peptide then folds in to form a six-stranded β sandwich. Within this structure, a groove between the βB strand and the αB helix is the binding site of the C-terminal peptide of the PDZ binding partner (Sheng and Sala, 2001). The four extreme C-terminal amino acid residues of the PDZ binding partner interact directly with this peptide-binding groove. The side chain of the C-terminal residue (position 0) projects into the hydrophobic pocket of the PDZ domain.

Therefore, most PDZ domains select for peptides with hydrophobic C-terminal residue such as valine, isoleucine, or leucine (Songyang et al, 1997). Generally, the PDZ recognition of position -1 residue of its C-terminal ligand is not very specific. It is the -2 position residue interaction with the first residue of α B helix (α B1 position) that determines the specific binding of the PDZ domain to certain peptides (Songyang et al, 1997). Based on the different types of this interaction, PDZ domains are divided to three classes.

The three classes of PDZ domain are defined by the -2 position amino acid residue of their binding partner. Class I PDZ domains select for a threonine or serine at the -2 position, the side chain of this amino acid forms a hydrogen bond with the histidine at the α B1 position. Class II PDZ domains are characterized by the hydrophobic residues found at both the -2 position of the C-terminal ligand and the α B1 position of the PDZ domain. Class III PDZ domains select for a negatively charged amino acid at the -2 position which interacts with the hydroxyl group of a tyrosine at the α B1 position (Songyang et al, 1997; Stricker et al, 1997). Although the -2 position of the C-terminal peptide residue is the most important position to determine the PDZ domain interaction with its ligand, residues at the -3 position also contribute to the interaction. Studies showed that residues at the -3 position also directly contact the peptide binding groove (Songyang et al, 1997).

Other than the interaction with the C-terminal peptides of its ligand, PDZ domains also bind to internal sequences of some proteins. They are able to form homo- or heteromultimers with other PDZ domains or other protein domains (Hsueh et al, 1997; Dong et al, 1999).

PDZ domains are often found in proteins containing other known interaction domains and signaling domains. The protein superfamily, membrane-associated guanylate kinases (MAGUKs), is one of the PDZ domain-containing protein families. The MAGUKs contain at least one PDZ domain, an Src homology 3 (SH3) domain and a guanylate kinase-like domain (GK). PSD-95, Dlg, and ZO-1 are examples of MAGUK proteins (Gonzalez-Mariscal et al, 2000). PDZ domains are also found in proteins containing domains such as LIM, calcium/calmodulin-dependent protein kinase-like domain and leucine-rich repeats (Hata et al, 1996; Cuppen et al, 1998; Bilder and Perrimon, 2000). Because of the diversity of PDZ domain-containing proteins, they are found in a lot of different protein complexes.

The major function of PDZ proteins is to act as scaffolds for the assembly of protein complexes. Scaffolding protein complexes containing PDZ proteins have been shown to function in synapse assembly, signal transduction, establishment of cell polarity and receptor localization. Details about some of these PDZ protein complex functions will be described in the following sections.

1.2 PDZ proteins and epithelial cell polarity

Cell polarity establishment and maintenance is very important for proper development and function of organisms. Two major cell types in which polarization is crucial for function are the neurons and epithelia (Roh and Margolis, 2003). In neurons, polarization occurs with the formation of the presynaptic and postsynaptic sites at the contacting neural cells. The pre- and postsynaptic membranes allow the directional action potential

and nerve impulse transmissions (Roh and Margolis, 2003). In epithelia, polarization occurs in the apicobasal axis. The epithelial membrane is divided into apical and basolateral compartments, which is important for cell morphology, tissue physiology and cell signaling (Bilder and Perrimon, 2000). The apical surface of a cell faces the external environment or a lumen, while the basolateral membrane is in contact with other cells and internal compartments. The basolateral membrane is subdivided into the basal domain that is defined by the cell-substrate adhesion and a lateral domain that is characterized by the cell-cell adhesion (Tepass et al, 2001). A central feature to determine the apical and basolateral membrane polarization is the localization of different proteins at different sites including the cell-cell junctions. One major focus of cell polarity studies is to analyze protein complex formation and interaction at the plasma membrane.

Drosophila embryos and mammalian cell lines are two major model systems for epithelial cell polarity research. In a polarized *Drosophila* epithelial cell, the lateral membrane can be roughly divided into three regions: the marginal zone (MZ), the zonula adherens (or the adherens junction) and the septate junction (SJ), from apical to basal, respectively. In vertebrates, the two major regions on the cell-cell contacting membrane is the tight junction (TJ) and zonula adherens (ZA), which is basal to TJ. Protein complexes assembled or molecules localized to these regions are intensely studied for they are important in establishing and maintaining the cell polarity and structure (Roh and Margolis, 2003). Recently, many studies have implicated PDZ domain containing proteins in cell polarity. Among them, three major protein complexes are believed to have significant roles in cell polarity establishment and maintenance.

The first PDZ protein-containing complex that is linked to cell polarity is the Bazooka (Baz)/*Drosophila* Par6 (Dpar6) /*Drosophila* homologue of atypical protein kinase C (DaPKC) complex. Both Baz and Par6 are PDZ proteins with Baz having three PDZ domains and DPar6 having one (Bilder, 2001). The mammalian homologues of these proteins have been identified, namely Par3/Par6/aPKC. In *Drosophila*, this protein complex is localized to the marginal zone of the lateral membrane, which is just above the zonula adherens and the ZA itself (Bilder et al, 2003). In mammals, this protein complex localizes to the tight junction, which is relatively at the same region as MZ in *Drosophila* epithelia.

The second protein complex that is involved in cell polarity is the Crumbs (Crb)/Stardust (Sdt)/Discs lost (Dlt) complex. Crumbs is a transmembrane protein that localizes at the apical surface membrane (Tepass et al, 1990). The four C-terminal amino acids of the cytoplasmic domain of Crb form a PDZ binding motif, which interacts with Sdt and Dlt, recruiting them to the apical region of lateral membrane. Both Sdt and Dlt are PDZ proteins. Sdt, a member of the MAGUK superfamily, contains a L27, a PDZ, a SH3, and a GK domain, while Dlt contains four PDZ domains and a putative MAGUK recruitment (MRE) domain (Roh et al, 2002). The mammalian homologues of Crumbs, Stardust, and Discs lost have also been identified. The homologue of Stardust is the Proteins associated with Lin-7 1 (Pals1), which gets its name from the association with mammalian Lin-7. Pals1, like Sdt, is a MAGUK protein, which has a similar domain structure as Sdt, but instead of one L27 domain, it has two, namely L27N and L27C. The L27C domain is the one that links Pals1 to mLin-7, while the L27N domain was found

recently to interact with a novel protein which was named the Pals1-associated tight junction (PATJ) protein. This PATJ protein was identified as a mammalian homologue of *Drosophila* Discs Lost (Roh et al, 2002). A recent study by Pielage and colleagues argued that the formerly known *Drosophila* homologue of PATJ, Dlt, is actually the product of another putative gene downstream to *dlt*, which is identified as CG12021 by the Berkeley *Drosophila* Genome Project (BDGP). Therefore, they suggested that to rename the gene *patj* as its vertebrate homologue (Pielage et al, 2003).

In *Drosophila* epithelia, the Crb/Sdt/Dlt (or PATJ) complex colocalizes with the Baz/DPar6/DaPKC complex to the marginal zone. Loss of *crb* function causes ZA disruption. Also, overexpression of Crb results in expansion of apical membrane to basolateral region (Tanentzapf and Tepass, 2002). These results suggest that Crb may be an important determinant for apical lateral surface.

The third protein complex involved in epithelial cell polarity is the Scribble (Scrib)/ Discs large (Dlg)/ Lethal giant larvae (Lgl) complex. The mammalian homologues of these proteins are Scrib/Vartul, mDlg/SAP97, and mLgl, respectively. Scrib is a PDZ domain containing protein that is consisted of 16 Leucine-rich repeats (LRR) and 4 PDZ domains (Bilder and Perrimon, 2000). Dlg is a MAGUK protein that contains three PDZ domains, one SH3 domain and one GK domain (Mathew et al, 2002). Lgl was originally identified in *Drosophila* as an epithelial tumour suppressor protein (Ohshiro et al, 2000). *scrib*, *dlg*, and *lgl* mutants show similar defects in epithelia, and these three proteins colocalize to the septate junction. Scrib is mislocalized in the absence of Lgl or Dlg, while Lgl is mistargeted when Dlg or Scrib is missing (Roh and Margolis, 2003). All

these results suggest that these three proteins form a complex and work in a common pathway, although there is no biochemical data to confirm the formation of this complex. In *scrib* mutant embryos, apical proteins such as Crb and adherens junctions are expanded to the basolateral membrane, but the basolateral membrane organization remains intact (Bilder and Perrimon, 2000). This result suggests that Scrib may act as a restriction to keep the apically localized proteins from expanding to the basolateral region.

Recent studies from Bilder and Tepass focus on the interaction between these protein complexes and have shed some light to the understanding of how these protein complexes function together to maintain cell polarity. From their studies, it seems that the initial step of polarization is the localization of the Baz complex to the apical region where the ZA assembly occurs. The localized Baz complex then targets the Crb complex to the marginal zone while the Scrib complex localizes to the region where SJ will be formed. The properly localized Scrib then acts to restrict the Crb complex at the apical region (Bilder et al, 2003; Tanentzapf and Tepass, 2003). Although epithelial polarity formation is becoming more clear, there are still questions to be answered. These protein complexes mentioned above are just a portion of a big group of proteins and molecules that are required for cell polarity establishment and maintenance. The understanding of the interactions and functions of all these proteins and molecules will provide a clearer picture of cell polarity mechanism.

1.3 PDZ protein at synaptic junction

Synapses are cellular junctions formed between neurons or neurons and their targets. A normal synapse consists of a presynaptic bouton, a synaptic cleft, and a postsynaptic reception area (Garner et al, 2000). A properly assembled synapse is required for normal signal transmission. The presynaptic bouton is where neurotransmitters are released, while the postsynaptic membrane is where neurotransmitter receptors accumulate to receive the signals. Both the presynaptic and postsynaptic compartments assemble protein complexes to maintain proper synaptic function. PDZ domain containing proteins have been identified to have important roles in synapse assembly including proper localization of postsynaptic neurotransmitter receptors and scaffolding for synaptic cellular adhesion molecules (Hata et al, 1998).

One major PDZ protein that is involved in synaptic assembly is the MAGUK protein family, which includes the *Drosophila* Discs large and its mammalian homologues PSD-95/SAP90, SAP97, PSD-93 and SAP102. Studies have shown that Dlg and PSD-95 are functionally important in ion channel and neurotransmitter receptor clustering and anchoring synaptic cellular adhesion molecules such as *Drosophila* Fasciclin II (FasII) through their PDZ domains or SH3 domains (Thomas et al, 1997; Tejedor et al, 1997; Zhang and Wang, 2003).

Drosophila Dlg is a MAGUK protein that contains three PDZ domains, one SH3 domain and a GK domain from its amino acid sequence N-terminal to C-terminal, respectively. Dlg has been showed to be important in epithelial cell polarity and synapse formation. A recent study showed that there are at least 5 isoforms of Dlg gene products.

Among the newly identified isoforms, a new protein domain has been described at the N terminus. This newly identified domain is termed S97N domain because it shares a 60% identity to the N-terminal 66 amino acids residues of SAP97 (Mendoza et al, 2003). Mendoza and colleagues showed that it is the newly identified Dlg isoform, S97N-Dlg, that is expressed in the nervous system and in the body wall muscles (where the neuromuscular junctions are formed). Mutations in S97N domain cause disruption in embryonic nervous system structure including loss of longitudinal and commissural patterns in the ventral cord and misrouting of axons (Mendoza et al, 2003).

The PDZ domains of Dlg have been shown to associate with cell adhesion molecules (CAM) such as FasII and ion channels such as Shaker K⁺ channel (Thomas et al, 1997; Tejedor et al, 1997). Cell adhesion molecules are important for appropriate synaptic connection. FasII belongs to the immunoglobulin superfamily of cell adhesion molecule (IgCAM). It is enriched at the growth cones of motor neurons during the axon pathfinding and then is expressed at the postsynaptic membrane as well after the proper formation of synapse (Schuster et al, 1996). Both *fasII* and *dlg* mutants cause an increase in the number of active zones at the presynaptic area (Thomas et al, 1997). Also, in *dlg* mutants the aggregation of FasII to synaptic membrane is decreased, which implies that Dlg regulate the distribution of FasII (Packard et al, 2003). The Shaker K⁺ channel is another interacting partner of the PDZ domains of Dlg. It was shown in a yeast two-hybrid experiment that the PDZ1-2 domain of Dlg bind directly to the C-terminal peptide of the Shaker protein. Dlg and Shaker colocalize to the postsynaptic membrane of the neuromuscular junction. In *dlg* mutant larvae that lack the first two PDZ domains,

Shaker was found to be diffusely distributed along the muscle membrane but not clustered at the junction (Tejedor et al, 1997).

In addition to the cell adhesion molecule, the PDZ domain of Dlg also interacts with the PDZ domain containing protein Scrib, which has an important role in maintaining epithelial cell polarity. Mathew and colleagues showed that other than its epithelial expression, Scrib is also found in the synapse and is localized to the synapse through the interaction with both Dlg and the novel Dlg binding protein GUKH (Mathew et al, 2002). Both interactions are PDZ domain mediated, where the C-terminal of Scrib interacts with the PDZ domain of Dlg and the PDZ domain of Scrib interacts with the C-terminal amino acid residues of GUKH (Mathew et al, 2002). It is believed that Dlg and GUKH work together to recruit Scrib to the synapse. *scrib* mutants in the synapse cause increased numbers of synaptic vesicles, abnormal vesicle distribution and a reduced active zone. It is suggested that Scrib is required to sustain synaptic vesicle concentrations at the site of release (Roche et al, 2002).

The GK domain of Dlg interacts with the novel Dlg binding protein GUK-holder (GUKH) as mentioned above. This interaction is mediated by an amino acid sequence motif near the C-terminal of GUKH. GUKH colocalizes with Dlg at the border of synaptic boutons (where the synapses are formed). However, the localization of GUKH to the synapse does not depend on Dlg, which suggests that other motifs of this protein are required for its synaptic localization. So far, the major function of GUKH identified is to recruit Scrib to the synapse through the cooperation with Dlg (Mathew et al, 2002).

1.4 The LIN-2/LIN-7/LIN-10 PDZ protein complex

Another the major function of PDZ proteins has been identified in sorting proteins such as receptors to proper locations. One example is the basolateral membrane localization of LET-23 by the tripartite protein complex, LIN-2/LIN-7/LIN-10, that was first identified in *C. elegans*. LIN-2 is a member of the MAGUK protein family, which contains a N-terminal Ca²⁺/calmodulin-dependent protein kinase (CaM kinase) domain, a LIN-7 binding domain (which is later termed L27 domain by Doreks et al [Doreks et al, 2000]), a PDZ domain, a SH3 domain, and a GK domain. LIN-7 is a small PDZ protein that contains a L27 domain and a PDZ domain. LIN-10 has a phosphotyrosine-binding domain (PTB) and two PDZ domains and has been identified as a binding partner of the glutamate receptor GLR-1 (Rongo et al, 1998). In *C. elegans*, loss of *lin-2*, *lin-7*, or *lin-10* activities result in a vulvaless phenotype, which is indistinguishable from the loss of *let-23* function phenotype (Simske et al, 1996). LET-23 is the *C. elegans* epidermal growth factor (EGF) receptor, which is required for the proper vulval development.

The *C. elegans* vulval development is controlled by the receptor tyrosine kinase (RTK) signal transduction pathway. During the third larval stage, the gonadal anchor cell produces an inductive signal that causes three of the six vulval precursor cells (referred to as Pn.p cells) to divide and form the vulva. The Pn.p cells are epithelial cells that line up in a row along the ventral midline (Simske et al, 1996). The signal that the anchor cell produces is Lin-3, a molecule that is similar to epithelial growth factor (EGF) and to transforming growth factor-alpha (TGF- α). This signal reaches the nearest Pn.p cell (usually the P6.p cell) and causes it to adopt the 1^o cell fate, which is for the precursor

cell to divide into 8 progeny that form the inner part of the developing vulva. This signal, along with other signals from the P6.p cell, induce the two neighboring cells (P5.p and P7.p cells) to adopt 2° cell fate. Therefore, each of the two cells generates 7 progeny that forms the outer part of the developing vulva. Finally, the other three Pn.p cells adopt the 3° cell fate, which is to divide once and then fuse with the hypodermis that forms the majority of the skin (Eisenmann and Kim, 1994). Even though most of the time it is the P6.p cell that adopts the 1° cell fate, each of the 6 precursor cells is competent to respond to the signal from the anchor cell. The receptor for the inductive signal (Lin-3) is LET-23, which is similar to receptor tyrosine kinase of the EGF receptor family. Therefore, it is believed that LET-23 binds to the signal, Lin-3, and then triggers the downstream transduction cascade to induce to vulva formation.

As mentioned above, mutations in *lin-2*, *lin-7* and *lin-10* show the same phenotype as mutation in *let-23*, which suggest that the three PDZ proteins are involved in the LET-23 signal transduction pathway. Since the three PDZ proteins as well as LET-23 are localized at the basolateral membrane in polarized epithelial cells and mutations in these genes show mislocalization of LET-23 to apical surface, it is speculated that the PDZ proteins are required for the proper localization of LET-23 to the basolateral membrane (Simske et al, 1996). Kaech and colleagues showed that the three PDZ proteins physically interact and form a tripartite complex that is required for the proper localization of LET-23 (Kaech et al, 1998). They first determined that the C-terminus of LET-23 is required for the basolateral localization. This C-terminal peptide resembles the type I PDZ binding motif. The single PDZ domain in LIN-7 is also a type I PDZ domain,

which was identified to bind to the C-terminus of LET-23. Mutations in the PDZ domain of LIN-7 and the C-terminus of LET-23 both mislocalize LET-23, therefore, this PDZ interaction is required for the proper localization of LET-23. In Kaech and colleagues' report, they also identified the interaction regions between the three PDZ proteins. The region between the N-terminal CaM kinase domain and the PDZ domain of LIN-2 binds to the N-terminal region of LIN-7 that has similar sequence. These regions were later named L27 domain since it was first found as the interacting domain between LIN-2 and LIN-7 (Doreks et al, 2000). The CaM kinase domain of LIN-2 interacts with a region upstream of the PTB domain of LIN-10. LIN-7 and LIN-10 do not physically interact. However, all three of them are required for the proper localization of LET-23 even though LIN-7 is the only one that binds to LET-23.

1.5 Mammalian homologs of LIN-2/LIN-7/LIN-10

LIN-2, LIN-7 and LIN-10 not only present in *C. elegans*, they are also found in mammals. Mammalian homolog of LIN-2, CASK, was identified originally as a neurexin interacting protein through a yeast-two-hybrid screen (Hata et al, 1996). Neurexins are neuronal cell adhesion molecules expressed in the presynaptic membrane, where they interact with the postsynaptic adhesion molecules, neuroligins, which in turn bind to another PDZ protein, PSD-95 (Irie et al, 1997). The structure of CASK is similar to its *C. elegans* homolog; there is an N terminal CaM kinase like domain, two L27 domains (L27N and L27C), a PDZ domain, a SH3 domain and a GK domain. Neurexin is not the only binding partner of CASK. Other known binding partners include syndecans, a

family of transmembrane heparon sulfate proteoglycans that colocalize with CASK at the synapse (Hsueh et al, 1998). Other than its synaptic expression, CASK is also expressed in epithelial basolateral membrane where it binds to the actin-binding protein band 4.1 (Cohen et al, 1998). Also, CASK associates with Parkin, an ubiquitin-ligase that is linked to Parkinson's disease, at the postsynaptic densities in the brain (Fallon et al, 2002).

Three forms of mammalian LIN-10 have been identified, they are named Mint1, 2, and 3. Mint1 and Mint 2 are neuron-specific proteins and were first identified as Munc 18 binding proteins (Okamoto and Sudhof, 1997). Munc 18 is a neuronal protein that is required for synaptic vesicle exocytosis, which is involved in neurotransmitter release. Mint 3 is a ubiquitously expressed protein; it shares similar C-terminal sequence with Mint 1 and Mint2, which contains a PTB domain and two PDZ domains, but it lacks the N-terminal Munc 18 interacting domain (Okamoto and Sudhof, 1998). Among the three isoforms, Mint 1 is the only one that binds to CASK. A recent study has shown that Mint 1 interacts with KIF17, a Kinesin superfamily motor protein, which is required for the transport of NR2B subunit of NMDA receptor (Setou et al, 2000). Also, it has been reported that Mints bind to Amyloid- β precursor protein (APP), which is implicated in Alzheimer's disease (Biederer et al, 2002).

Mammalian LIN-7s were originally identified by two different groups which respectively named them Veli (for vertebrate lin-7) and Mals (for mammalian homologs of lin-7) (Butz et al, 1998; Jo et al, 1999). Three isoforms of mammalian LIN-7 were identified by these two groups, which will be referred to as Veli-1, -2, and -3 from this point on. Veli-1 and Veli-2 are brain specific while Veli-3 is most abundantly expressed

in kidney but is found in every tissue tested such as brain, liver, thymus and heart (Jo et al, 1999). These mammalian LIN-7s were found to form a tripartite protein complex with CASK and Mint 1 as their *C. elegans* homologs. The interactions are the same as in *C. elegans*, that is, L27 domain of Velis bind to the L27C of CASK (Harris et al, 2002) and CASK binds to a N-terminal region of Mint 1 by its CaM kinase domain (Butz et al, 1998).

Velis have been found to interact with a lot of proteins. MAGUK proteins other than CASK were linked to Velis through the L27 domain. PALS-1 is one of the MAGUK proteins that bind to Velis, it is, as mentioned above, important in cell polarity maintenance in the epithelial cells. Another MAGUK protein that was found to interact with Velis is called VAM-1, whose function is not clearly known, but is speculated to function in cell-cell junction, too (Tseng et al, 2001).

Also, Velis have been suggested to interact with other proteins through the PDZ domain. In Jo and colleagues' research, they found that Velis bind to the C terminus of NR2B subunit of NMDA glutamate receptor and colocalize with PSD-95 at the postsynaptic density (Jo et al, 1999). Velis have been found to associate with β -catenin at the cell-cell junctions of both neurons and epithelial cells through their PDZ domains (Perego et al, 2000). Perego and colleagues also showed that the PDZ domain of Velis bind to the epithelial γ -aminobutyric acid (GABA) transporter (BGT-1); this interaction is required for the basolateral membrane retention of BGT-1 in the epithelial cells, that is, mutants without this interaction cause BGT-1 internalization (Perego et al, 1999). Velis are also linked to ion channels such as the Kir 2.3 channel, a potassium channel, in renal

epithelia. This interaction is also PDZ mediated and is required for proper localization of Kir 2.3 channel to the basolateral membrane (Olsen et al, 2002). They have also been linked to the nectin-afadin based cell-cell junction and are independent to the catenin-cadherin system, however, Velis were not found to directly interact with nectin or afadin (Yamamoto et al, 2002).

Finally, like their *C. elegans* homolog, Velis are also found to interact with the mammalian EGF receptor, ErbB-2. As in the *C. elegans* interaction, the PDZ domain of Velis bind to the C-terminal of Erb-2 and is responsible for its basolateral localization. However, in Shelly and colleagues' report, they identified a new motif of Veli called KID, which locates at the N-terminal of Veli, upstream of L27 domain (Shelly et al, 2003). This newly identified motif is responsible for delivery of ErbB-2 to the basolateral membrane while the PDZ interaction is important for keeping ErbB-2 there.

Unlike *C. elegans* LIN-2/LIN-7/LIN-10 complex, mammalian homologs of these proteins seem to be involved in many different functions according to all the known binding partners and localization of these protein. Figure 1 shows the summarized interactions of these proteins in mammals that were mentioned above. CASK, Velis, and Mints can form a tripartite protein complex and recruit neurotransmitter receptors to the PSD as reported by Jo et al (Jo et al, 1999). They can also pair up as in the case of basolateral membrane localization of the potassium channel Kir 2.3 mediated by hLin-7b/CASK complex (Olsen et al, 2002). They can also function in other protein complexes that do not relate to each other. Although many interacting partners of these

proteins have been identified, the functions of these proteins remain unclear and need further genetic studies to understand them.

1.6 *Drosophila* homologs of LIN-2, LIN-7, and LIN-10

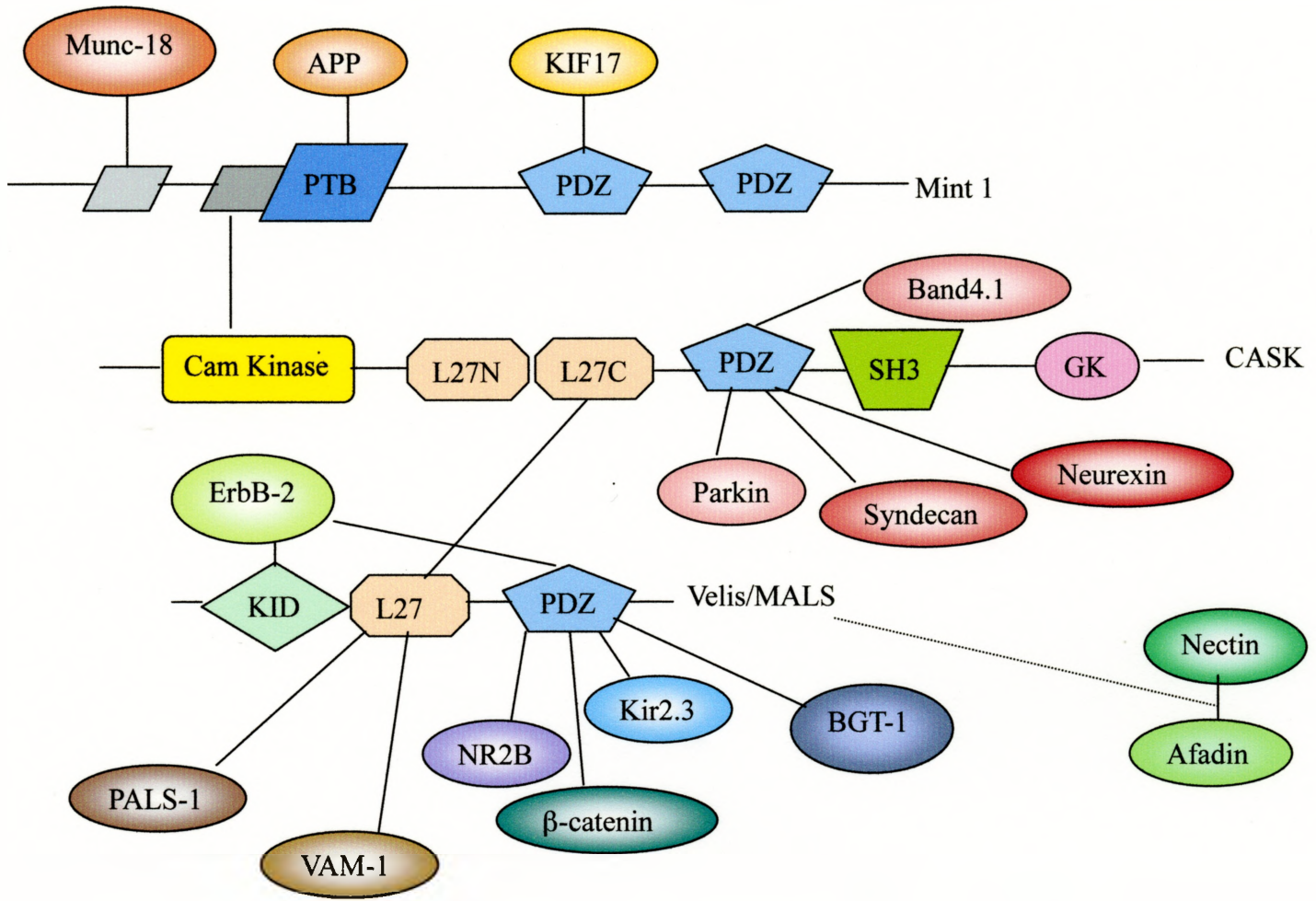
The ease of genetic manipulation and the fully sequenced genome make *Drosophila* an excellent experimental model organism for both genetic and biochemical studies. The *Drosophila* homologs of LIN-2, LIN-7 and LIN-10 were identified. The *Drosophila* ortholog of *lin-2/Cask* was first identified by different groups and was named as *Camguk* (*cmg*) and *Caki*, respectively (Dimitratos et al, 1997; Martin and Olo, 1996). *Camguk* is highly expressed in the central nervous system throughout the developmental stages, suggesting a neuronal role (Lopes et al, 2001). Mutant analysis of *Caki* also shows reduced walking speed in adult flies, which supports a role of this protein in synapse function (Martin and Olo, 1996).

Drosophila homolog of LIN-10/Mint was identified by different groups through genomic analysis and was known as CG5675, CG5678 and Mint in Flybase (Flybase ID: FBgn0026313). It is now named X11L in Flybase and was isolated and characterized by Hase and colleagues. It is expressed in the neuronal tissues from late embryonic to adult stage and was found to interact with APP as its mammalian homologs (Hase et al, 2002).

The *Drosophila lin-7/veli* cDNA was isolated in Dr. Jane McGlade's laboratory (University of Toronto, Canada) in a screen for protein containing a PDZ domain. The initial study showed this protein binds to phosphorylated *Drosophila* EGFR (DER). It was then sent to Dr. Roger Jacobs' laboratory and was characterized by Allison

Figure 1. Proteins interact with CASK, Velis and Mints

The domains of CASK, Velis and Mints are indicated in this figure. Proteins that interact with different domains of them are also shown in the figure. Solid line indicates direct interaction while dotted line means indirect interaction. Although the protein interactions shown in this figure are found in mammalian cells, many of them have homologs in invertebrates and the interactions have been identified in invertebrate system, too.



MacMullin and named *dveli* for *Drosophila veli* (MacMullin, 2001). The coding region of *dveli* is 585 base pairs long and encodes a 195 amino acids peptide that contains two known protein domains, a L27 domain and a PDZ domain. The newly identified KID domain of its mammalian homolog has not been identified in dVELI. After the publication of *Drosophila* genome sequence, a BLAST search of the *dveli* cDNA revealed that the gene CG7662 of BDGP corresponds to *dveli*. dVELI shows higher homology to its mammalian homologs than the *C. elegans* LIN-7. For example, dVELI has a 68% sequence identity with *C. elegans* LIN-7 and 80% identity with rat VELI-C. It was mapped to the 96B16 region of right arm of third chromosome in *Drosophila* genome (MacMullin, 2001). *in situ* hybridization studies showed that *dveli* transcripts are expressed mostly in the larval CNS neuron somas. It is also expressed at lower levels in larval imaginal discs (MacMullin, 2001). Western blot analysis shows that dVELI is expressed in larval and adult tissues, but not in embryos (MacMullin, 2001). Immunohistochemistry tests show the temporal and spatial distribution of dVELI. Antibody staining showed that dVELI is abundant within the neuropil of the larval ventral ganglion and also within the mushroom bodies of the brain (MacMullin, 2001). Both areas are sites of synaptic connection. Larval neuromuscular junction (NMJ) staining showed that dVELI localises mostly to the post-synaptic density (MacMullin, 2001). Expression of dVELI is also observed in the brain of the adult fly. Because of the similarity in structure, sequence and expression pattern to the mammalian homologs, it was hypothesized that dVELI functions in a complex with CAMGUK and X11L, which is required for proper localization of receptors to the post-synaptic density of neurons.

A recent report by three groups of researchers from CuraGen Corporation, Wayne State University, and Yale University proposed a protein interaction map of *Drosophila melanogaster*. A mass Yeast two-hybrid screen using all known or predicted transcripts (10,623 in total) against DNA libraries was done, and they produced a draft map of 7048 proteins and 20405 interactions (Giot et al, 2003). Among these interactions, dVELI was found to interact with EGFR as it was originally identified in McGlade's lab. It was also identified to interact with Skiff, a guanylate kinase containing a SH3 domain and a PDZ domain. Other than these two known genes, *dveli* was also identified to interact with three putative genes, CG10176, CG11208, and CG9326. CG9326 shows a 39% amino acid identity to PALS2 (proteins associated with LIN-7 2), which was identified from an assay for mLin-7 interacting proteins (Kamberov, 2000; MacMullin, 2001). *camguk* and *XIII* were not found to interact with *dveli* in this draft map. However, the interactions showed in this map may not be entirely reliable since some known interactions were not found. For example, the only interaction with the *Drosophila Egfr* identified in this map is *dveli*, but it has been reported to interact with at least 76 other genes (Flybase ID FBgn0003731). It is highly unlikely that the gene product only binds to dVELI. Therefore, to identify proteins that really interact with dVELI, a more detailed study is required.

1.7 *Drosophila* as a model organism to study function of VELI

Drosophila is an excellent experimental model system. The ease of genetic manipulation, the well-defined ultrastructure, and the fully sequenced genome make it a great model organism to study genetic interaction and *in vivo* gene product relations. Also, as surprisingly as it seems, *Drosophila* show a close conservation of many genes identified in mammals (Koh et al, 2000), even though it is a much simpler organism in structure. Therefore, it is among the most valuable model systems for examining the molecular and cellular basis of many protein functions. Although a lot of proteins that interact with Veli have been identified in the mammalian system, most of them lack *in vivo* interaction and physiological function studies. Since dVELI has high sequence and structure homology to Veli and also the expression pattern is similar, the study of *dveli* should provide a more clear view of *veli* functions *in vivo*.

The focus of this thesis will be first to create mutants of *dveli* and then to analyze dVELI function in the synapse. The mutagenesis method used in this thesis will be the P element mobilization method. If dVELI is required for proper localization of receptors in synapse as hypothesized, a loss of function mutant might reduce synaptic output or delay the signal transduction. Therefore, phenotypes such as locomotion behaviour changes, paralysis, and even lethality might be observed. Also, misexpression studies using the UAS-GAL4 expression system will be done to attempt to determine the normal dVELI function. By using different neuronal and muscle GAL4 drivers, it is hoped that possible dominant negative or gain-of-function effects will result from overexpression and provide insight to the function of dVELI in pre- and post-synaptic area differentiation. Another

method to study the function of the gene that will be used is the RNA interference technique. A systemic RNAi approach adopted from the protocol of Dr. Davis' laboratory is used (Eaton et al, 2002). It is speculated that by interfering with gene expression with double stranded RNA, loss of function phenotypes such as slower locomotion or lethality will be observed.

Chapter 2

Materials and Methods

2.1 *Drosophila melanogaster* Strains

Drosophila melanogaster strains used includes the following: *CS-P* (Canton S-P element free), $P\{w^{+mc}=\text{lacW}\}OstStt3^{2D9}$, $w^{-};+;Dr/TMS \Delta 2-3 Sb$, $w^{-};+;ry^{506} Sb \Delta 2-3/TM6 Tb$, $yw; Sco/CyO$, $Df(3R)96B$, $Df(3R)XTA1$, *Slit 1.0 lacZ*, $yw; +; D/TM3 Sb$ and *yw*. All strains were obtained from Bloomington Stock Center.

CS-P is a wild type control strain. The P element line, $P\{w^{+mc}=\text{lacW}\}OstStt3^{2D9}$, contains a P element insert upstream of *dveli* at the 5' end of the gene *OstStt3*. Two transposase source lines, $w^{-};+;Dr/TMS \Delta 2-3 Sb$, and $w^{-};+;ry^{506} Sb \Delta 2-3/TM6 Tb$, were used for P element mobilization to generate mutants. The second chromosome balancer line, $yw; Sco/CyO$, was used to map the UAS *Lin7* constructs insertions. $yw; +; D/TM3 Sb$ is a third chromosome balancer line which was used in P element mutagenesis. Two deficiency lines, $Df(3R)96B$ and $Df(3R)XTA1$, which lack the 96B1-11 region and 96A17-21 to D1, respectively, were used for complementation tests. And the *Slit 1.0 lacZ* line was used for β -galactosidase activity assay.

2.2 Embryo, larva and adult fly collection

Adult flies are kept in plastic vials containing autoclaved yeast *Drosophila* food medium. Embryos were collected using "houses" that contain adult flies. The houses are 100ml plastic beakers with holes at the bottoms to allow adequate air flow. Adult flies

were collected, put into the houses, and the open end of the houses were secured with Petri dishes filled with apple juice agar (2.25% (w/v) agar, 2.5% (w/v) sucrose, 25% (v/v) apple juice). Adult flies would lay eggs on the apple juice agar plates and the embryos were collected. The agar plates were changed and then incubated at 18°C or 25°C with different time periods to obtain embryos at different stages. Different stages of larvae were collected using a similar method. Instead of apple juice agar, the Petri dishes were filled with food medium. After the embryos were collected on the food plates, the plates were then incubated at 25°C for different time periods to obtain different stages of larvae. First instar larvae were obtained approximately 24 hours after embryos hatched. Second instar larvae took about 48 hours, the foraging stage of third instar larvae were collected about 94-96 hours after the embryo hatching. 96-110 hour old larvae are the wandering stage of third instar larvae.

2.3 P element mutagenesis

One P { $w^{+mc}=\text{lacW}$ } *OstStt3*^{2D9} P element transposon line, which has the transposon construct located about 4kb away from *dveli* was used to try to create mutants by P element local mobilization. Two different transposase source lines were used: $w^{-};+;Dr/TMS \Delta 2-3 Sb$, and $w^{-};+;ry^{506} Sb \Delta 2-3/TM6 Tb$. Several steps of crosses were done as illustrated in Figure 5. First step was to cross the transposon line to the transposase lines, the progenies of this cross (F1) would contain both transposon and the transposase which would cause the P element to move in the germ line. The next step was to get rid of the transposase source so the P element would be stable within the genome. Next, the

potential mutant alleles are crossed back to the original P element insert line to test for complementation. The ones that complemented with the original insertion are the ones that have P element insertion somewhere else in the genome (Grigliatti, 1998). These lines were then kept over the balancer chromosome *TM3* to prevent chromosomal recombination. The next step was to test for the lethality of these potential alleles by self-crossing. The ones that are homozygously lethal were then crossed to the deficiency lines to test for the locations of the P element insertions. The ones that failed to complement with the deficiency were the ones that have insertions located within the deficiency region. The genetics scheme for the deficiency screen is illustrated in Figure 6 in the results section.

2.4 Confirmation of original P element insertion by PCR

PCR was used to verify the location of the P element insert in the $P\{w^{+mc}=\text{lacW}\}OstStt3^{j2D9}$ line. Three sets of primers were used, with one forward inverse primer (p primer: 5'-GACGGGACCACCTTATGTTATTTTCATCATG-3') designed at the terminal inverse repeat of the P element and three reverse primers: one at the 3' end of *OstStt3* (2 primer: 5'-ATGTACACTCTGCTTTATTGAATTGCTAGC-3'), one at the 5' end of *dveli* (1 primer: 5'-TACCACACCATTACAGACAAAAGTTGATCT-3') and one at the 3' end of *dveli*, the P2 primer (5'-ATGGGCCCCATTTATGGACTGAACTTATGAAG-3').

By the size of the amplified fragments from these primer sets, the location of the P element insert was determined.

2.5 Preparation of genomic DNA for PCR screen

About 200 adult flies were collected and left in a clean plastic vial for 1 to 2 hours at room temperature. Then the flies were ground in liquid nitrogen with pre-cooled mortar and pestle. The ground flies were then transferred to a cooled dounce homogenizer containing 2 ml of homogenization buffer (10mM Tris-HCl pH7.5, 60mM NaCl, 10mM EDTA, 0.15mM spermidine, 0.15mM spermine). The ground flies were homogenized in the buffer to free cells from the fly tissues. The homogenized solution was transferred to microcentrifuge tubes and centrifuged at 1000rpm for one minute to remove the debris. The supernatant was collected and centrifuged again at 8000 rpm for 5 minutes. The pellet was collected and resuspended in 0.5 ml homogenization buffer. Then proteinase K was added to the solution to a final concentration of 100µg/ml and 1 to 2 µl of 10 mg/ml RNase A was added as well. 50µl of 10% SDS was added to the solution, then it was mixed by swirling and rocking. The mixture was then incubated at 37°C for 45 to 60 minutes. After the incubation, an equal volume of phenol was added and mixed with the mixture, then it was centrifuged at 10000 rpm for three minutes in 4°C. The top layer was transferred to a new tube, then an equal volume of chloroform was added and mixed with it. The mixture was centrifuged at 10000rpm for three minutes, the top layer which contains the DNA was transferred to a new tube. 1/10 volume of 3M NaAc and 2.5 volume of chilled absolute ethanol were added. The mixture was kept in -20°C for 20

minutes. Then it was centrifuged at 12000 rpm for 20 minutes at 4°C. The pellet was washed in 70% ethanol and then centrifuged again. The ethanol was then removed. After the pellet was dried, it was dissolved in ddH₂O.

2.6 UAS-GAL4 Misexpression

Three UAS LIN-7 lines, UAS LIN-7a, UAS LIN-7b and UAS LIN-7c, were constructed by Allison MacMullin in Dr. Jacobs' lab. They were mapped by crossing to *Sco/CyO*. LIN-7(dVELI) was misexpressed by crossing to several GAL4 lines: *24B* GAL4, *twist* GAL4, *c179* GAL4, *en* GAL4, *elav* GAL4, *sim* GAL4, *ey* GAL4, *sevenless* GAL4, *pGMR* GAL4, *scabrous* GAL4 and *hs* GAL4. Embryos from these crosses were collected on apple juice agar plates. Then the embryos were counted and lined up in the middle of the plate and were kept in the room temperature or at 25°C for two days. After the two-day incubation time, the percentage of unhatched embryos was counted and calculated as viability values. First instar or third instar larvae were collected and put in fly food medium containing yeast, the percentage of larvae that developed to pupae and then adult flies was calculated and recorded as larval viability.

2.7 Generation of dVELI-His fusion construct

dveli cDNA without stop codon was amplified with PCR by using the forward primer containing NdeI restriction enzyme site and the reverse primer containing HindIII cutting site using a pBluescript KSII-*dveli* plasmid made by Allison MacMullin as template. The PCR product was first cloned into the pCR2.1 vector by using the TA cloning kit

(Invitrogen, #45-0046). By using the X-gal selection system, the colonies that had inserts were picked and tested with restriction enzyme digestion. Once the insertion was confirmed, the insert fragment was cut out of the vector with NdeI and HindIII, and then subcloned into the pET29b+ vector (Novagen, #69872-3), which contains a C-terminal His-tag sequence. Then the plasmid was transformed into the bacterial host strain BL21- λ DE3. The ligation was confirmed by restriction enzyme digestion and PCR using the two primers to amplify the insert fragment.

2.8 Expression of dVELI-His fusion protein

Bacterial culture was inoculated in LB medium containing Kanamycin (final concentration 30 μ g/ml) till the optimal concentration (O.D.₆₀₀~ 0.6) was reached. Then 0.1 mM IPTG (final concentration) was added to induce the protein expression. Bacterial cells were collected by centrifugation at 10000g for 10 minutes. The pellet was resuspended in lysis buffer (150mM NaCl, 50mM Tris, 1% Triton X100, pH8.0) and then lysed by sonication. After sonication, the cell debris was collected by centrifugation and the supernatant containing the crude protein extract was kept in -80°C for further use.

2.9 Purification of dVELI-His fusion protein

Ni-CAMTM HC resin (Sigma, #N 3158) was used to purify the dVELI-His fusion protein. First, 1 ml of resin was transferred to a Poly-prep chromatography column (BioRad, #731-1550). Let the beads settle down in the column. The resin was washed with two column volumes of deionized water, followed by three column volumes of

equilibration buffer (50mM sodium phosphate, 0.3M sodium chloride, 10mM imidazole, pH8.0). After the washes, load the crude protein extract onto the column and then wash the column with 10 to 20 column volumes of wash buffer (50mM sodium phosphate, 0.3M sodium chloride, 10mM imidazole, pH8.0). Each fraction of the washes was monitored by measuring the O.D.₂₈₀ values using the spectrophotometer. The washes continued until the O.D.₂₈₀ values were stable and near that of the wash buffer. Finally, the His-tagged protein was eluted from the column using 3 to 10 column volumes of elution buffer (50mM sodium phosphate, 0.3M sodium chloride, 250mM imidazole, pH8.0). The eluted fractions were collected and analyzed with SDS-PAGE for the target protein. Then the eluted fraction that contained the target protein was dialyzed against coupling buffer (0.1M NaHCO₃, 0.5M NaCl, pH8.3). After the elution, the column was washed with 2 volumes of ddH₂O followed by five volumes of 6M guanidine HCl (pH 7.5). Then the column was washed with 3 column volumes of ddH₂O. Finally, the column was washed with 20% ethanol and stored at 4°C for further use.

2.10 Preparation of dialysis tubing

The tubing was cut into appropriate size, and then was boiled for 5 minutes in dialysis tubing buffer (5mM EDTA, 200mM NaHCO₃). Then the tubes were rinsed with deionized water. These tubes were boiled in the buffer and rinsed with deionized water again. Then the tubes were put in large amount of water and autoclaved. After they cooled down, the tubes were stored in the autoclaved water at 4°C for further uses.

2.11 Affinity purification of dVELI antibody

dVELI antibody was purified using the CNBr-activated sepharose 4B (Amersham Biosciences, # 17-0430-01). First, the beads were swollen in 1mM HCl for 15 minutes. Then the swollen gel was washed on a sintered glass filter with 1mM HCl (use 200ml HCl/ g of dry beads) followed by 5 volumes of coupling buffer (0.1M NaHCO₃, 0.5M NaCl, pH8.3). Next, incubate the His-tagged dVELI protein (in coupling buffer) with the gel at a 2:1 ratio overnight at 4°C with rotation. The next day, the gel coupled with the antigen was washed with 5 volumes of coupling buffer. After the wash, add 0.1M Tris-HCl (pH8.0) to block remaining active group on the gel for two hours at room temperature. Then the beads were poured into the BioRad Poly-prep chromatography column (BioRad, #731-1550). After the beads settled down in the column, it was washed with 5 to 10 column volumes of 1X PBS. Then the serum obtained from rat with five boosts of GST-DVELI injection (MacMullin, 2001) was added to flow through the column by gravity flow, the serum was cycled through the column several times. After the antibody bond to the antigen, the column was washed several times with 1X PBS. Then the antibody was eluted with 0.2M glycine (pH2.3). The eluted antibody was neutralized with 1M Tris buffer (150µl per ml of eluted solution), then it was dialyzed against 1X PBS overnight at 4°C. Add 0.02% sodium azide to the antibody and store it at -80°C.

2.12 Immunostaining of larval central nervous system

Third instar larval CNS (central nervous system) was dissected in cold 1X PBS, then the nervous system was fixed in 4% paraformaldehyde in sodium phosphate buffer (pH7.4) for 1 to 2 hours at room temperature. The fixed larval CNS was washed in 1X PBT (1X PBS with 0.3% triton) for two hours on a rotator with several changes of PBT. The tissues were then blocked with NGS (1:20 dilution) in PBT for 40 minutes to eliminate non-specific binding. Then primary antibody was added at desired dilution in PBT. The tissues were incubated in primary antibody overnight at 4°C. Next day, the tissues were washed 5 times with PBT, and were rotated in PBT for 2 hours with several changes of buffer. After the washes, the tissues were blocked in NGS again, then they were incubated in HRP conjugated secondary antibody for two hours at room temperature. After the incubation, the tissues were washed again in PBT for 1 to 2 hours on a rotator with several changes of PBT. The buffer were removed after the washing period, then PBT containing 0.33 mg/ml of DAB was added to the tissues for 2 minutes, then 3 μ l of 0.03% H₂O₂ was added. The reaction was stopped until desired coloration was achieved with PBT washes. Then the tissues were washed in 1X PBS and stored in 70% glycerol in PBS.

2.13 Preparation of crude protein from *Drosophila* tissue

Adult fly tissue was collected and homogenized in cold RIPA lysis buffer (150mM NaCl, 1% NP-40, 0.5% deoxycholate, 0.1% SDS, 50mM Tris-HCl pH8.0). Protease inhibitor cocktail tablet (Roche, # 1836170) was added to the buffer before use. 2 ml of

RIPA buffer were used for 1 g of tissue. After homogenizing, the samples were incubated on ice for ten minutes. Then they were centrifuged for five minutes at 3500 rpm. The supernatant containing the protein were collected and stored at -80°C for further use.

Larvae were collected and homogenized in 1X SDS lysis buffer (50mM Tris-HCl pH6.8, 2% SDS, 10% glycerol, 100mM β -mercaptoethanol) in a 1:2 ratio (1 volume of larvae with 2 volume of buffer). Protease inhibitor cocktail tablet was added to the buffer before use. Then the homogenized tissue was boiled for 5 minutes at 95°C and was vortexed for 30 seconds. Following the vortexing, the samples were centrifuged at 4°C for 10 minutes. The supernatant containing the protein were collected and stored at -80°C for further use.

2.14 Protein concentration determination

Bradford method was used to determine protein sample concentration. BioRad Protein Assay Dye Reagent (Bio-Rad, # 500-0006) was used for the measurements. The dye reagent was diluted in deionized water (1part of reagent with 4 parts of water), and was filtered through Whatman filter paper (Cat. # 1001125) to remove particulates. Then 1 μ l of protein sample was added to 2 ml of the dye reagent and was mixed well by vortexing. The samples were measured using a spectrophotometer at 595nm wavelength. O.D.₅₉₅ values of bovine serum albumin (BSA) at various concentrations were measured and used as protein standards. A standard curve was plotted using the absorbance values and known concentrations of BSA, a linear relation should have shown between the O.D.

values and the concentrations. The concentrations of the samples were then calculated from the standard curve using the formula obtained from the linear line.

2.15 Western Blot analysis

30 to 50 μ g protein sample were mixed with 3 μ l 5X SDS loading buffer (60mM Tris-HCl [pH6.8], 25% glycerol, 2% SDS, 0.1% biomophenol blue, 5% 2-mercaptoethanol) and boiled for five minutes at 95°C to denature the proteins. The samples were then loaded on to 12% SDS-PAGE gel and run at 120V for 90 minutes. After running the gel, the proteins were transferred to BioTrace™ PVDF membrane (Pall life sciences, P/N 66543) in transfer buffer (15.6mM Tris, 120mM glycine, 20% methanol, 0.02% SDS) at 4°C. After the transfer, the membrane was blocked with 5% skim milk in post blotting buffer (154mM NaCl, 10mM Tris-HCl pH7.4) for one hour at room temperature. Then the membrane was incubated overnight in primary antibody with appropriate dilution factor in the blocking solution at 4°C. The next day, the membrane was washed three times with post blotting buffer containing 0.05% NP-40 to remove excess primary antibody. After the washing, the membrane was incubated in an HRP-conjugated secondary antibody solution with appropriate dilution for 40 to 60 minutes at room temperature. Then the membrane was washed twice again with post blotting buffer containing NP-40, followed by two washes with 10mM Tris-HCl (pH7.4). Finally the membrane was prepared for autoradiographic developing using Kodak X-ray film. The membrane was incubated in equal amount of reagent 1 mixed with reagent 2 from ECL™ Western Blotting detection Kit (Amersham BioSciences, # RPN2106) for 3 minutes. The

membrane was placed in transparent sheet and exposed to Kodak X-OMAT AR film (Kodak, REF# 165-1454) in the dark for various time periods and developed for the signal of antibody labeling.

2.16 Preparation of double stranded RNA template constructs

The construct for making *dveli* double stranded RNA (ds *dveli*) was generated by Dr. Chun mei Wang. *dveli* cDNA was subcloned into the LITMUS 28i vector from the HiScribe™ RNAi Transcription Kit (New England Biolabs # E2000S). The construct for making *lacZ* double stranded RNA was generated with the same method. A fragment of *lacZ* gene (bp3090-3835 Gen Bank accession #J01636) was amplified with PCR using the forward primer containing BglII restriction enzyme site and reverse primer containing PstI. The PCR product and LITMUS 28i vector were then digested with the restriction enzymes. After the digestion, the fragment and the vector were ligated together using the T4 DNA ligase (Invitrogen) in several different insert/vector ratio reactions. The ligation products were transformed into the bacterial host strain DH5 α and was spread on LB plates with Ampicillin (final concentration 100mg/L). Several colonies were picked up the next day and cultured in LB medium containing Amp. The bacterial cells were collected and the plasmid DNA were extracted using the QIAprep Spin Miniprep kit (Qiagen, #27104). The DNA was then subjected to restriction enzymes digestion for verification of the inserts. The ones that contain the right insert size were sent for sequencing and were blasted against the NCBI database for confirmation of correct *lacZ* fragment insertion. Once the insertion is confirmed, the plasmid was used to generate the

template for making double stranded RNA. LITMUS 28i vector contains two opposing T7 promoters flanking the multiple cloning sites, when the constructs were subjected to PCR using T7 promoter primer, a fragment of *dveli* (or *lacZ*) containing two T7 promoter on either sides was generated. This fragment of DNA would be used as the template for *in vitro* transcription for double stranded RNA.

2.17 *in vitro* transcription of double stranded RNA

in vitro transcription of *dveli* and *lacZ* double stranded RNA were done using the protocol from the HiScribe™ RNAi Transcription Kit. The reaction mix includes RNase-free water, 10X Transcription buffer containing 5mM NTPs, ~ 0.5µg template DNA, 30X HMW mix and 150U T7 RNA polymerase. After mixing, the reaction mix was incubated in 42°C for three hours and then was heated to 65°C for 5 minutes to improve efficiency of strand annealing. Then the reaction was cooled down to room temperature. Once the reaction mix was cooled down, the double stranded RNA was purified with phenol/chloroform extraction and then was dissolved in RNAi solution (6% sucrose, 5X Spradling buffer [25mM KCl, 50mM NaH₂PO₄ pH7.8]). The concentration of purified double stranded RNA was estimated with the O.D.₂₆₀ value obtained from the spectrophotometer. For O.D.₂₆₀ value equals one, the concentration is estimated as 45µg/ml. After the determination of the concentration, purified double stranded RNA was kept in -20°C for further use.

2.18 RNAi Soaking Technique

This technique is modified from Davis Lab Larval RNAi Soaking Technique. *CS-P* adult flies and *Slit1.0 lacZ* reporter flies were collected and put in houses. The embryos of these flies were collected on Apple Juice Agar plates for 2 hours and allowed to develop till 18-20 hours old before the feeding. Once the embryos were old enough, they were dechorinated with 50% bleach (diluted with DEPC treated deionized water), and then were soaked in 20 μ l of RNAi solution (purified double stranded RNA, 6% sucrose, 5X Spradling buffer [25mM KCl, 50mM NaH₂PO₄ pH7.8]) for 14-16 hours at room temperature. After the soaking, the larvae were picked up and transferred to food plate till they develop to third instar larvae. The third instar larvae were then used for behavior tests or β -galactosidase activity assay.

2.19 Quantitative β -galactosidase activity assay

Ten to fifteen third instar larvae were collected and homogenized in microcentrifuge tubes containing 100 μ l assay buffer (50mM potassium phosphate buffer, 1mM MgCl₂, pH7.5). Then add 900 μ l assay buffer and mix by vortexing for 30 seconds. Centrifuge at 8000 rpm for one minute to remove the tissue. Then the protein concentration was measured using Bradford assay. After measuring the protein concentration, transfer an aliquot of the crude extract to a cuvette containing 1 ml of CPRG solution (1mM CPRG [Chlorophenol Red β -D-galactopyranoside] in assay buffer). The solution was incubated at 37°C with absorbance checked at 574nm for every half an hour over a two hour period. β -galactosidase activity was calculated as O.D.₅₇₄ value/hour/mg of protein.

2.20 Larval locomotion behavior assay recording and measurement

Larval locomotion behavior assay was done using the Semi-automated tracking system designed by Balaji Iyengar from Dr. Campos' lab. The tests were done under a "safe-light" condition, which is using a 20W incandescent lamp fitted with Kodak GBX-2 filter as the light source (Iyengar, 2002). This light source would emit a red light with wavelength above 600nm, which could not be detected by the larvae, therefore would not interfere with the larva behavior. Third instar larvae survived from the RNAi soaking were tested for locomotion behavior. Larvae were picked from the food plate, cleaned in water, and then transferred to 1% agar plates for behavior test. The larvae were allowed to get familiar with the new environment for one minute, and then the images of the larvae were captured by a CCD video camera (Elmo 272s), which is connected to a Mac G3 computer. The image of the larva was seen on the computer screen and the locomotion of the larva was tracked manually using a Stylus pointing at the larva posterior and moving on a Wacom Intuos Tablet connected to the computer. The program for tracking was written as a macro used in NIH Image program by Balaji Iyengar. The positions of the larvae were recorded for 30 seconds. Then the distances that the larvae moved were calculated. Statistics were done on the recorded values then the results were compared among the different test groups.

Chapter 3

Results

dveli was isolated by the McGlade lab at the Sick Children Hospital in Toronto during a search for PDZ domain binding proteins using fly expression libraries (MacMullin, 2001). It was characterized by Allison MacMullin in the Jacobs lab of McMaster University. Based on the results from her experiments, dVELI contains a single PDZ protein motif that is often found in scaffolding proteins. It also contains a L27 domain that likely allows it to bind to CAMGUK (Kaech et al, 1998). *in situ* hybridization studies showed that *dveli* is expressed mostly in the CNS neurons of the larva and adult. In the larval CNS, dVELI is localized to the neuropil areas of the ventral nerve cord and brain. The neuropil contains most of the synaptic connections in the CNS. Western blot analysis showed that dVELI could be found in larval and adult tissues, but not in embryos. Neuromuscular junction (NMJ) staining showed that dVELI localises mostly to the post-synaptic density. Based on these results, we hypothesize that dVELI functions in a complex with CAMGUK and dMINT required for proper localization of receptors to the post-synaptic density in neurons. In this thesis work, mutant generation and analysis of dVELI function will be studied.

3.1 P element insertional mutagenesis

The first method used to generate mutants of *dveli* is the P element mutagenesis method. P element was originally discovered as a mobile genetic element that is associated with spontaneous mutations in nature (Rubin et al, 1982). There are two types of P element; the complete (or autonomous) P element is 2907 bp long with four exons, the defective ones (or nonautonomous) contain internal deletions of the complete and the sizes vary with the deletions. One major characteristic of P element is that it contains a 31 bp inverted repeat sequence at both ends (O'Hare and Rubin, 1983), which is important for the mobilization. The complete P elements translate into two types of protein: the 87 kDa transposase and the 66 kDa repressor (Rio et al, 1986). Since the defective P elements contain internal deletions that would disrupt the translation of the 87 kDa protein, which cause them immobile, this 87 kDa product was named transposase for that it is important for the P element mobility.

Base on the characteristics of P element structure, a mutagenesis method is developed. Two types of P element constructs were generated. One is called the transposase, which is a P element missing one or both terminal repeat regions but stably encodes the 87 kDa transposase protein. This type of P element construct is not able to move due to the lack of the terminus. The second type is the transposon construct that contains a visible or selectable marker within a defective P element. The transposon is stable in the genome unless a transposase is provided. When a transposon line is crossed to a transposase line, the progeny would have mobile P element within the germline, which may result in change of P element locations. P element can cause mutation by

either insert into genes or by imprecise excision from genes (Grigliatti, 1998). The method used in this thesis work is the insertional mutagenesis.

Confirmation of original P element insertion

The P element insertion used in this thesis work is $P\{w^{+mc}=\text{lacW}\}OstStt3^{j2D9}$, in which a P element transposon construct, P [lacW], is inserted at the 5' end of the gene *OstStt3* (Flybase). The P [lacW] construct is a modified P-element transposon, which contains the eye-color marker w^{+mc} , a *lacZ* reporter gene, and a plasmid replicon with a poly-linker. The marker allows for the selection of the P element construct. To confirm the insertion of the P element line, a PCR method was used. A forward primer (P primer) designed at the terminal inverse repeat of the P element and a reverse primer at the 3' end of *OstStt3* (2 primer) were used for the PCR amplification. Figure 2 shows the schematic of this method. Figure 3 shows the result of the PCR, a fragment with the size of approximately 2.9Kb was amplified. The amplified fragment was then sent to Mobix lab of McMaster University for sequencing. The sequence was aligned with the sequence of *OstStt3* obtained from NCBI database using the program ClustalW. Figure 4 shows the sequence alignment. The alignment shows 95% identity, the errors may be due to sequencing error or PCR errors. With the correct amplified fragment size and the 95% sequence identity, the insertion of the P element in the $P\{w^{+mc}=\text{lacW}\}OstStt3^{j2D9}$ fly line was confirmed.

Figure 2. Schematic of the PCR method for confirming P element insertion

The figure shows the position of the primers used in this method. The forward primer (P primer) is at the terminal inverse repeat of P element, the reverse primer (2 primer) is at the 3' end of *OstStt3*. The gene size is approximately 2.9Kb. The relative position of the genes and the gene sizes were based on the *Drosophila melanogaster* chromosome 3R, section 88 of 118 complete sequence obtained from NCBI database (accession number, AE003750).

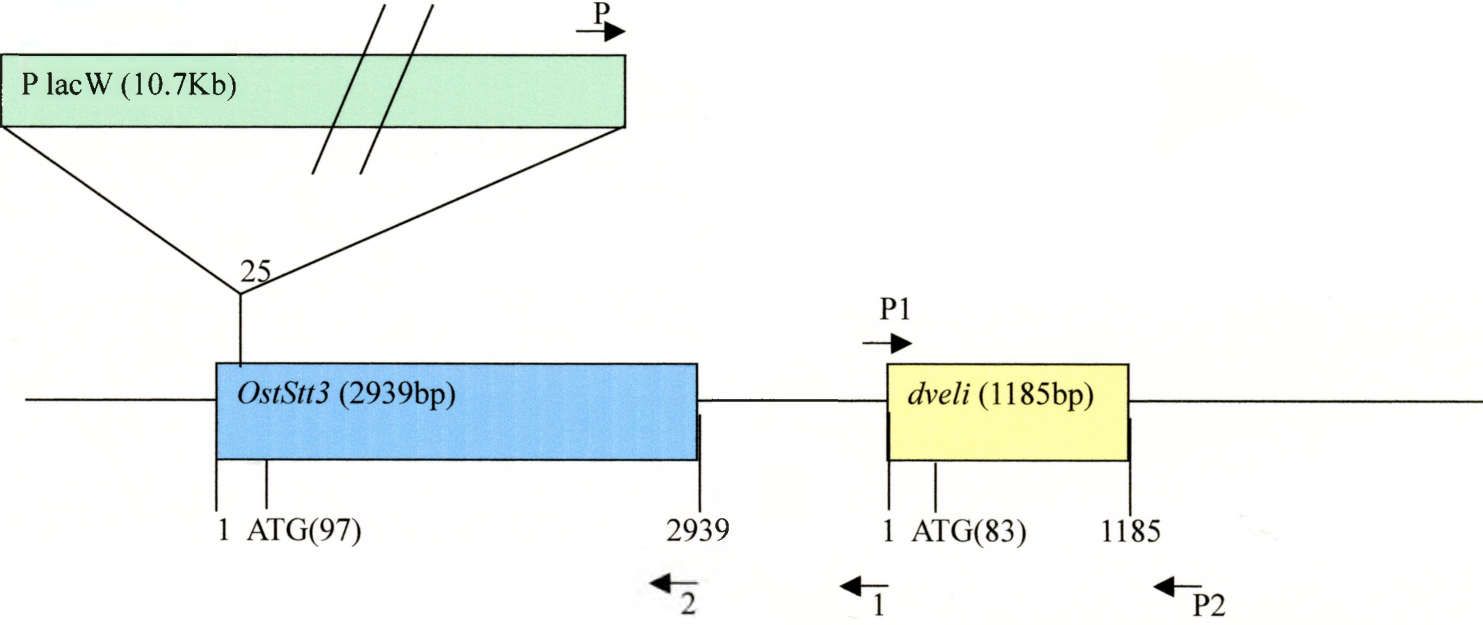


Figure 3. PCR result

The template used was the genomic DNA prepared from the $P\{w^{+mc}=\text{lacW}\}OstStt3^{j2D9}$ adult flies. Two different template concentrations were tested: 1000 ng and 100 ng. The amplified fragments were run on a 0.8 % agarose gel with a 500bp DNA ladder (Invitrogen).

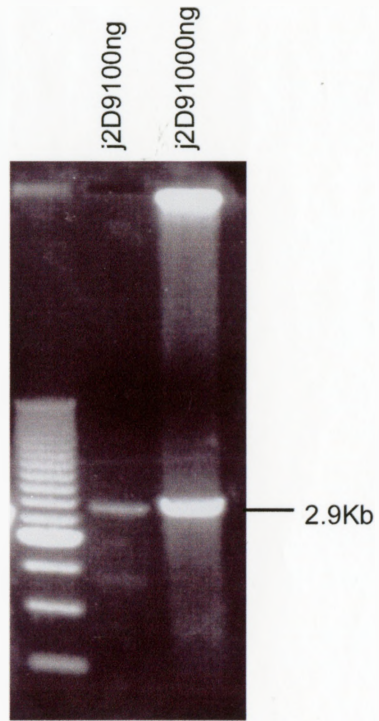


Figure 4. Sequence alignment

The PCR products were sequenced and aligned with the *OstStt3* sequence (NCBI accession # NM_079770). Sequencing was done using forward primer (P), about 1061 bp were sequenced. The alignment showed 95% identity.

OstStt3 j2D9p	ACCCGGCAATTTTT-TTAGACTACGTGTCTAAGCGAAGAATGTGTCGTTGCATTTAGAT --TAGGCNATTTCCATTAAAAGGCCAGGGNGTGTGANATAAGGGGNGCC---CTTAATGT	59 55
OstStt3 j2D9p	CGGTTATAATTTTCGAGTTACTGGCTGGAATTGGGACATG-AATCGGACGCCGAAG-ATG ATGCGA-GNTACTTGAGACGTGGG--AATCTGGGTACATGGAATCGGACGCCGAAGGATG	117 112
OstStt3 j2D9p	CTGAACAGCAA-GGTGGCTGGCTACAGCAG--CCTAATCACCTTCGCCATCTGCTAATC CTGAACAGCAAAGGTGGCTGGCTACAGAAGGCCCTAATCACCTTCGCCATCTGCTAATC	174 172
OstStt3 j2D9p	GCCTGGCT-GGCCGGATTTTCTCTCGCCTCTTCGCCGTCATCCGTTTCGAGTCGATTAT GCCTGGCTTGGCCGGATTTTCTCTCGCCTCTTCGCCGTCATCCGTTTCGAGTCGATTAT	233 232
OstStt3 j2D9p	CCATGAGTTTGATCCGTGGTTCAACTACCGGGCCACCGCCTACATGGTGCAGAATGGTTG CCATGAGTTTGATCCGTGGTTCAACTACCGGGCCACCGCCTACATGGTGCAGAATGGTTG	293 292
OstStt3 j2D9p	GTACAACCTCCTCAACTGGTTCGACGAGCGCGCATGGTATCCGCTCGGCAGGATTGTGGG GTACAACCTCCTCAACTGGTTCGACGAGCGCGCATGGTATCCGCTCGGCAGGATTGTGGG	353 352
OstStt3 j2D9p	CGGTACCGTCTATCCCGCCTGATGATTACGTCCGGCGGAATCCATTGGCTGCTGCACGT CGGTACCGTCTATCCCGCCTGATGATTACGTCCGGCGGAATCCATTGGCTGCTG-ACGT	413 411
OstStt3 j2D9p	ACTCAACATACCGGTCCATATTCGTGACATCTGCGTGTTCCTGGCGCCGATCTTCAGTGG ACTCAACATACCGGTCCATATTCGTGACATCTGCGTGTTCCTGGCGCCGATCTTCAGTGG	473 471
OstStt3 j2D9p	CCTGACCTCCATCTCCACCTACCTGCTGACCAAGGAGCTGTGGTCCGCGGGCGCCGGCCT CCTGACCTCCATCTCCACCTACCTGCTGACCAAGGAGCTGTGGTCCGCGGGCGCCGGCCT	533 531
OstStt3 j2D9p	CTT-CGCCGCCAGCTTCATCGCCATCGTGCCTGGCTACATCAGTAGGTCGGTGGCTGGAT TTTTCGCCGCCAGCTTCATCGCCATCGTGCCTGGCTACATCAGTAGGTCGGTGGCTGGAT	592 591
OstStt3 j2D9p	CGTACGATAACGAGGGCATTGCCATATTCGCCCTGCAGTTCACCTACTTCTGTGGGTGC CGTACGATAACGAGGGCATTGCCATATTCGCCCTGCAGTTCACCTACTTCTGTGGGTGC	652 651
OstStt3 j2D9p	GCTCAGTGAAGACTGGATCCGTGTTCTGGTCGGCCGAGCCGCTTTGTCTACTTCTACA CCTCAGTGAAGACTGGATCCGTGTTCTGGTCGGCCGAGCNGTTTTGTCTACTTCTACA	712 711
OstStt3 j2D9p	TGGTGTCCGCTGGGGTGGCTACGTGTTTCATCATCAACCTGATACCCCTGCACGTCTTCG TGGGNCCGCTGGGGTGNCTACGTGTTTCATNATCAACCTGATNCCNTGCACGTNTTCG	772 771
OstStt3 j2D9p	TACTGCTCATTATGGGCAGGTACTIONCGCCGGTCTGCTGACCAGCTACAGCACCTTCTACA GACTGCTNATTATGGGCAGGNACTIONCGCCGGTTTGNTGAC-AGCTANAG-ACCTNTACA	832 829
OstStt3 j2D9p	TCCTGGGACTGCTGTTCTCCATGCAGATCCCCTTCGTGGGATTCGAACCGATACGCACCA TCCTGGNACTGNTGT-CTCCATN-AGATCCCTTC---GGGGATTCNACCGAT-CCCACAG	892 883
OstStt3 j2D9p	GTGAACACATGGCTGCGCTGGGAGTGTGTTGTGCTCCTTATGGCCGTGGCCACCTTGCGCC GNAAA---ATGGNTNNN-TGGGAGTTTTNGN---TCTTATGGCG--GGCCNNTGGCA--	952 932
OstStt3 j2D9p	ATTTGCAGTCCGTGCTGTGCGCAACGAGTCCGGAAGCTGTTTCATCGTCGGCGGATTGC --TTNNAGNCCG-GCTG--GCNCNACNGNT--CGGAGCTTAAATGTCGCGGATTN--TGN	1012 983
OstStt3 j2D9p	TGGTGGGCGTTGGCGTCTTTGTGGCCGTCGTGGTGTCTACCATGCTGGGCGTTGTGGCCC NGCTTTGCNTTTTGGCCNCGGGGGCTACATCTGNGTTNGGCCCGGGAGGGACNTCTACTC	1072 1043
OstStt3 j2D9p	CGTGGAGTGGACGCTTCTACTCGCTGTGGGATACTGGCTACGCCAAGATCCACATTCCCA TTGGGANTGNTNCCAAAT-----	1132 1061

Genetics of P element mobilization

P element mutagenesis was used to try to create mutant alleles of *dveli*. The transposon, P{w^{+mc}=lacW} *OstStt3*^{2D9}, was used for P element mobilization mutagenesis. *OstStt3* or Oligosaccharyl transferase 3, which has oligosaccharyl transferase activity, is located about 1.1Kb upstream of *dveli* (FlyBase cytologic map). The P element transposon construct, P[lacW], is inserted at the 5' end of *OstStt3*, and the insertion is located about 4.1Kb from the start codon of *dveli*. This P element insert is a lethal allele of *OstStt3* according to Flybase data. Since the P element is close to *dveli*, it is possible to mobilize the P element to insert even closer to *dveli*, which might interrupt the promoter region of the gene, or the P element might insert right inside the gene and hence interrupt the gene function.

The transposon is stabilized in the genome unless a transposase source is provided. In this experiment, two transposase lines were used: w⁻;+;Dr/TMS Δ2-3 Sb and w⁻;+;ry⁵⁰⁶ Sb Δ2-3/TM6 Tb. Figure 5 shows the genetic scheme of this P element mobilization. First step is to cross the transposon to the transposase lines, the progeny of this cross would contain both the mobile P element and the transposase, therefore the P element would be able to move around in the genome. Once the P element is moved, the next step is to remove the transposase so the P element inserts would be stabilized in the genome. After the removal of transposase, the next step is to cross the potential alleles to the original P element insert line for complementation test. 159 of 1137 lines were identified being hopped out of the original P element insertion because they complemented to the original P element line. Among these 159 lines, 122 are homozygously lethal and 37 are non

lethal. These potential mutants are kept over the balancer *TM3* to prevent recombination. After mapping the location of the P element insertion with *yw; Sco/CyO*, 107 of the homozygously lethal lines and 31 of the non-lethal lines were found to be on the third chromosome, the rest were on second chromosome.

Deficiency screen

After obtaining all these potential mutants, the next step is to determine the location of the insertion. First a deficiency screen was done. A deficiency line, *Df(3R)XTA1*, which lack the whole 96B region on the third chromosome, was used for complementation test. This deficiency line is kept over a duplication, *Dp(3;3)M95A⁺13*, and both chromosome lack dominant markers to differentiate them. Therefore, a control cross was tested first to find out if both *Df(3R)XTA1* and *Dp(3;3)M95A⁺13* over the balancer *TM3* are viable and hence are differentiable by the recessive marker *ebony*. Figure 6 shows the genetic scheme of this deficiency test. After the deficiency test, only 21 lines of the 107 lethal lines fail to complement the deficiency line, which means they are located within the region of the deficiency and possibly within or close to *dveli*. The results of deficiency screen are summarized in Appendix 8.

Figure 5. Genetics of P element mobilization

Step 1 is to cross P element line to the transposase, the genotype in the red square is the one that is being selected, which is the one has both P element and transposase. This cross is done in *en masse*. Step 2 is to get rid of the transposase so the mobilized P element will be stable in the genome. This step is done in pairwise crosses because at this point the P element insertion in each fly may be at different locations. Also, male flies containing the P element inserts were used to avoid chromosomal recombination. Step 3 is the complementation test to the original P element insert line, if $yw;+;P?/P\{w^{+mC}=lacW\}OstStt3^{j2D9}$ survive (P? stands for the new insertion that the location of the P element insert is unknown), new inserts complement the original one, which means the P element moved, then male and female of $yw;+;P?/TM3, Sb^1$ flies from the same tube are selected and self-crossed to keep a stock of these potential alleles. Step 4 is to self-cross the potential alleles to keep a stock of them and to test for lethality. If $yw;+;P?/P?$ survives, the insert is non-lethal, if not, the insert is homozygously lethal.

Step 1 *en masse* cross

$$y^1 w^{1118};+; P\{w^{+mC}=lacW\}OstStt3^{j2D9}/TM3, Sb^1 \times w^*;+; ry^{506} Sb^1 P\{ry^{+17.2}=\Delta 2-3\}99B/TM6B, Tb^1$$

$$\Downarrow$$

$$P\{w^{+mC}=lacW\}OstStt3^{j2D9}/ry^{506} Sb^1 P\{ry^{+17.2}=\Delta 2-3\}99B$$

$$yw/w \text{ or } yw/Y \text{ or } w/Y;+; P\{w^{+mC}=lacW\}OstStt3^{j2D9}/TM6B, Tb^1$$

$$; TM3, Sb^1 / ry^{506} Sb^1 P\{ry^{+17.2}=\Delta 2-3\}99B$$

$$; TM3, Sb^1 / TM6B, Tb^1$$

Step 2 pairwise cross

$$yw/Y \text{ or } w/Y;+; P\{w^{+mC}=lacW\}OstStt3^{j2D9}/ry^{506} Sb^1 P\{ry^{+17.2}=\Delta 2-3\}99B \times yw;+;D/TM3, Sb$$

$$\Downarrow$$

$$P?/D$$

$$yw/Y \text{ or } yw \text{ or } yw/w;+; P?/TM3, Sb$$

$$; ry^{506} Sb^1 P\{ry^{+17.2}=\Delta 2-3\}99B/D$$

$$; ry^{506} Sb^1 P\{ry^{+17.2}=\Delta 2-3\}99B/TM3, Sb$$

Step 3 pairwise cross

$$yw/Y;+;P?/D \times y^1 w^{1118};+; P\{w^{+mC}=lacW\}OstStt3^{j2D9}/TM3, Sb^1$$

$$\Downarrow$$

$$yw;+;P?/ P\{w^{+mC}=lacW\}OstStt3^{j2D9} \longrightarrow \text{the survival of this genotype indicate the}$$

$$;P?/ TM3, Sb^1 \qquad \qquad \qquad \text{complementation test result}$$

$$;D/ P\{w^{+mC}=lacW\}OstStt3^{j2D9}$$

$$;D/ TM3, Sb^1$$

Step 4 pairwise cross

$$yw/Y;+;P?/ TM3, Sb^1 \times yw/yw;+;P?/ TM3, Sb^1$$

$$\Downarrow$$

$$yw;+; P?/P? \longrightarrow \text{the survival of the genotype indicate the lethality status of this allele}$$

$$; P?/ TM3, Sb^1$$

$$; TM3, Sb^1 / TM3, Sb^1$$

Figure 6. Genetics scheme of deficiency screen

The deficiency line used in this screen is

Df(3R)XTA1,th¹ st¹ kni^{ri-1} rn^{roe-1}p¹/Dp(3;3)M95A⁺13,st¹ e¹ (Bloomington Stock Center #2366). The break point of this deficiency line is 96A17-21;96D1, therefore, the entire 96B region is missing in the deficiency line. A control cross is done first to determine if the deficiency and the duplication are viable over the balancer *TM3*. The result shows that the numbers of the phenotypes Normal body, non-*Sb*: normal body, *Sb*: black body, *Sb* (*Sb* is a dominant marker which shows shorter hairs on the ventral part of the adult fly) = 427:133:149 which is close to 3:1:1 rather than a estimated 2:1:1 ratio. Therefore, *Df(3R)XTA1/TM3* and *Dp(3;3)M95A⁺13/TM3* are both viable but weaker. Then the potential mutant alleles are crossed to the deficiency line. If P? lies within the deficiency region, then the ratio of the phenotypes normal body, non-*Sb* : normal body, *Sb*: black body, *Sb* should be 1:1:1, otherwise the ratio should be close to 2:1:1

After testing all 107 potential insertion lethal lines, only 21 of them have ratio close to 1:1:1 (the results are summarized in Appendix 8).

Control Cross:

<u>Df(3R)XTA1, th st kni rn p</u>		<u>+</u>		
<u>Dp(3;3)M95A⁺13, st e</u>	X	<u>TM3 Sb e</u>		expected proportion
		↓		
<u>Df(3R)XTA1, th st kni rn p</u>			normal body color, non-Sb	25%
+				
<u>Df(3R)XTA1, th st kni rn p</u>			lethal? normal body color, Sb	25%
<u>TM3 Sb e</u>				
<u>Dp(3;3)M95A⁺13, st e</u>			normal body color, non-Sb	25%
+				
<u>Dp(3;3)M95A⁺13, st e</u>			black body, Sb	25%
<u>TM3 Sb e</u>				

Deficiency screen:

<u>Df(3R)XTA1, th st kni rn p</u>		<u>P?</u>		expected proportion	
<u>Dp(3;3)M95A⁺13, st e</u>	X	<u>TM3 Sb e</u>		P? within	P? not in
		↓		deficiency	deficiency
<u>Df(3R)XTA1, th st kni rn p</u>			lethal?	0%	25%
P?					
<u>Df(3R)XTA1, th st kni rn p</u>			normal body color, Sb	33%	25%
<u>TM3 Sb e</u>					
<u>Dp(3;3)M95A⁺13, st e</u>			normal body color, non-Sb	33%	25%
P?					
<u>Dp(3;3)M95A⁺13, st e</u>			black body, Sb	33%	25%
<u>TM3 Sb e</u>					

PCR screen

After the deficiency screen, a PCR screen was attempted to try to locate the exact location of the P element inserts. The PCR screen scheme is similar to the PCR method used to confirm the original P element insertion in the $P\{w^{+mc}=\text{lacW}\}OstStt3^{j2D9}$ line. A forward primer (P primer) which is designed at the terminal inverse repeat of the P element and three reverse primers (2 primer, 1 primer and P2 primer) were used to identify the location of the insertion. 2 primer is designed at the 3' end of *OstStt3*, 1 primer is designed at the 5' end of *dveli* and P2 primer is designed at the 3' end of *dveli*. These three sets of primers were used to determine the location of the potential alleles. With different sizes of amplified PCR fragments, the location of the P element inserts should be able to be determined.

Figure 7 shows the schematic of this PCR screen. The genomic DNA of the original P element insertion line, $P\{w^{+mc}=\text{lacW}\}OstStt3^{j2D9}$, was used as the template to test these three sets of primers and as positive control for every PCR screen. The set of P and 2 worked on every trial, the set of P and 1 worked occasionally, the set of P and P2 didn't work. The reason the PCR didn't work may due to the difficulty of amplify long fragments (4 Kb for P and 1, and 5.2 Kb for P and P2) or bad designs of the primers. Another forward primer (P1 primer), which is designed at the 5' end of *dveli*, is used together with P2 primer to amplify *dveli*, this amplification is used as a control for testing the genomic DNA preparation. Table 1 shows the PCR screen results of some of the potential alleles. 25 out of 52 tested lines show that the P element has moved out of *OstStt3* since there were no fragments being amplified using P and 2 primers. 10 of these

25 lines do not have the P element inserted in the region between *OstStt3* and *dveli* because there were no fragments being amplified by P and 1 primers. Due to the time constraint, the PCR screen could not be completed in this thesis work. The PCR screen is currently continued in Dr. Jacobs lab by Dr. Firoz Mian.

Figure 7. Schematic of PCR screen

Three sets of primers are used for determining the location of the P element insert. One forward primer (P primer) at the terminal inverse repeat of P element, and three reverse primers: 2 primer at the 3' end of *OstStt3*, 1 primer at the 5' end of *dveli* and P2 primer at the 3' end of *dveli*. With different locations of the P element inserts, the fragment amplified by these primer sets would be different, hence the location of the P element should be able to be determined. In the figure three possible insertion locations are illustrated. If P element inserted somewhere more downstream in *OstStt3* (a), the primer set P and 2 should amplify a fragment less than 2.9Kb. If the transposon is inserted in between the two genes (b), the primer set P and 1 should amplify a fragment less than 1.1Kb. If it is inserted somewhere within *dveli* (c), a fragment less than 1.2Kb should be amplified by P and P2. Another set of primers (P1: 5'-CACGGAATGGTATTTTGTGCCCTGAGACG-3' and P2: 5'-ATGGGCCCCATTTATGGACTGAACTTATGAAG-3') were used to amplify *dveli*. This is used as a positive control for the template condition. The fragment amplified by P1 and P2 should be about 1.2 Kb.

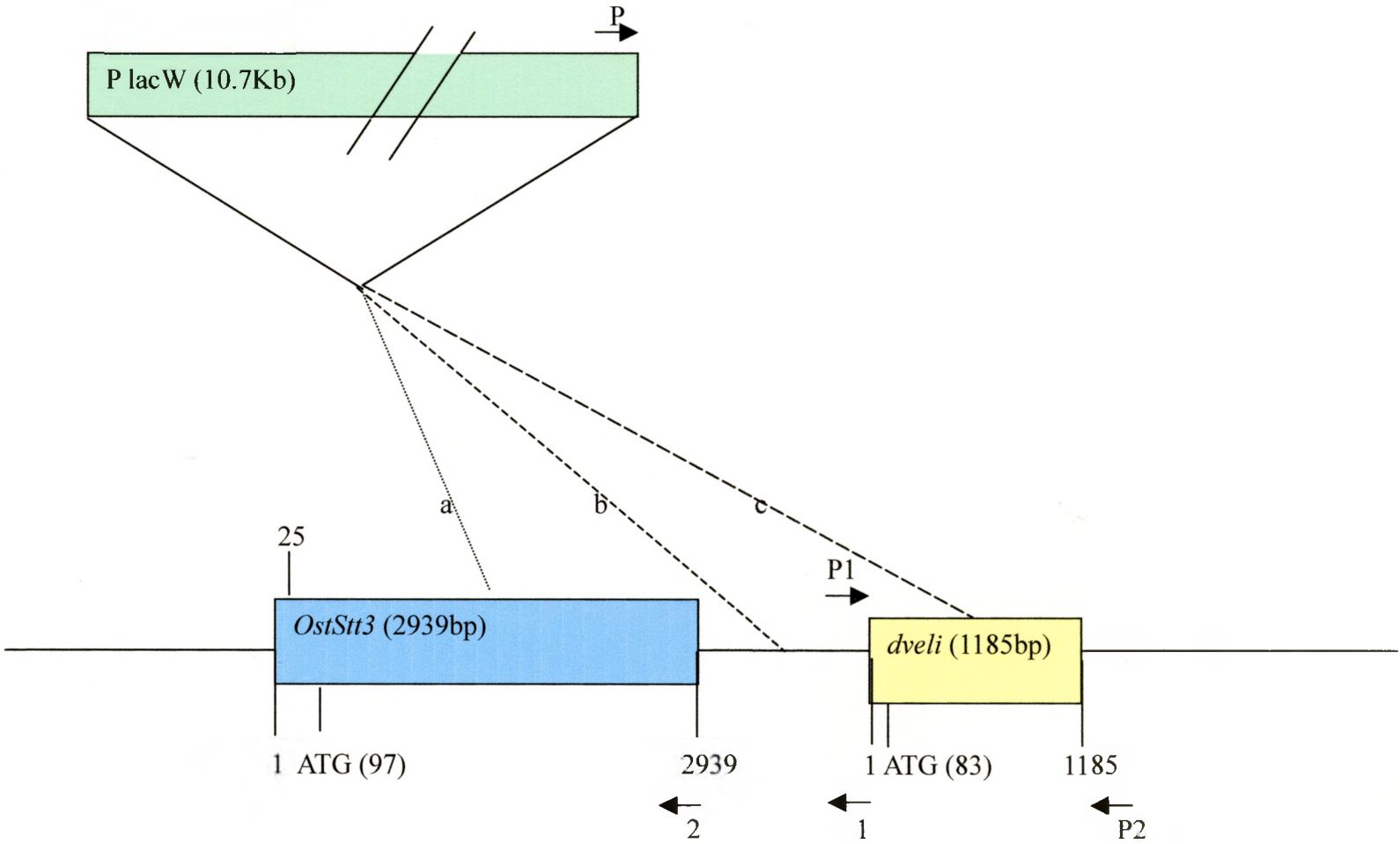


Table 1. PCR screen result

Homozygously lethal lines				Non-lethal lines			
Line#	P1 P2	P 2	P 1	Line#	P1 P2	P 2	P 1
P71	1.2kb	X	X	O57	1.2kb	X	
P19	1.2kb	X		O30	1.2kb	X	
Q31	1.2kb	X		O29	1.2kb	X	
G57	1.2kb	X		O52	1.2kb	X	
O50	1.2kb	X		P9	1.2kb	X	
E29	1.2kb	2.9kb		P70	1.2kb	X	
Q65	1.2kb	2.9kb		N39	1.2kb	X	
P6	1.2kb	2.9kb		O67	1.2kb	X	
C62	1.2kb	2.9kb		O68	1.2kb	X	
<i>Q37</i>	<i>1.2kb</i>	<i>X</i>	<i>X</i>	O38	1.2kb	X	
<i>P1</i>	<i>1.2kb</i>	<i>X</i>	<i>X</i>	G17	1.2kb	2.9kb	
<i>O27</i>	<i>1.2kb</i>	<i>X</i>	<i>X</i>	N13	1.2kb	2.9kb	
<i>J39</i>	<i>1.2kb</i>	<i>X</i>	<i>X</i>	O18	1.2kb	2.9kb	
<i>J46</i>	<i>1.2kb</i>	<i>X</i>		P17	1.2kb	2.9kb	
<i>Q32</i>	<i>1.2kb</i>	<i>X</i>		J34	1.2kb	2.9kb	
<i>N23</i>	<i>1.2kb</i>	<i>X</i>		I4	1.2kb	2.9kb	
<i>N22</i>	<i>1.2kb</i>		<i>X</i>	P60	1.2kb	2.9kb	
<i>O55</i>	<i>1.2kb</i>		<i>X</i>	Q59	1.2kb	2.9kb	
<i>R7</i>	<i>1.2kb</i>		<i>X</i>	O69	1.2kb	2.9kb	
<i>K28</i>	<i>1.2kb</i>	<i>2.9kb</i>		R5	1.2kb	2.9kb	
<i>G18</i>	<i>1.2kb</i>	<i>2.9kb</i>		I10	1.2kb	2.9kb	
<i>P68</i>	<i>1.2kb</i>	<i>2.9kb</i>		O23	1.2kb	2.9kb	
<i>N10</i>	<i>1.2kb</i>	<i>2.9kb</i>					
N56	1.2kb	X	X				
J12	1.2kb	X	X				
N12	1.2kb	X					
L16	1.2kb	X					
O28	1.2kb	X					
O46	1.2kb	X					
Q46	1.2kb	X					

X = no fragment being amplified

Blank = no test result available

Bold letter = lines fail to complement deficiency line

Italic letter = lines complement deficiency line

3.2 Purification of dVELI antibody

dVELI antibody is needed for confirmation of dVELI protein production in various experiments including the misexpression of *dveli* at various tissue types and determination of the RNA interference effects. Rat serum containing dVELI antibody was generated by Allison MacMullin using a GST-dVELI fusion protein as antigen (MacMullin, 2001). Due to the loss of the GST-dVELI fusion protein construct, a dVELI-His fusion protein construct was made by using the whole *dveli* cDNA excluding stop codon and the pET29b+ vector (Novagen) to purify the antibody. The fusion protein was purified using the Ni-CAM resin from Sigma and then coupled to CNBr-activated Sepharose 4B beads. Serum containing dVELI antibody was loaded to the column to bind to the immobilized antigen (dVELI-His fusion protein), and then was purified with glycine washes.

Analysis of the purified antibody

The purified antibody was tested on wild type adult fly whole protein extract using a Western Blot analysis. A band of approximately 24 KDa should be detected if the purified antibody is working. Figure 8 shows the result of the Western Blot analysis. A band of size of dVELI (~24KDa) was detected as expected. The purified antibody was tested on wild type larval CNS as well by immunostaining. Figure 9 shows the result of the immunostaining. The staining showed that dVELI expression is located in the brain lobe and nerve cord as expected (MacMullin, 2001).

Figure 8. Western Blot analysis of CS-P adult fly whole protein

CS-P adult fly whole protein extract were prepared as mentioned in Method. It was loaded on a 12% SDS-PAGE gel and then transferred to the membrane. The primary antibody used was the purified dVELI antibody with two different dilution factors (1:500 and 1:1000). Bands with the size approximately 24KDa were detected as expected.

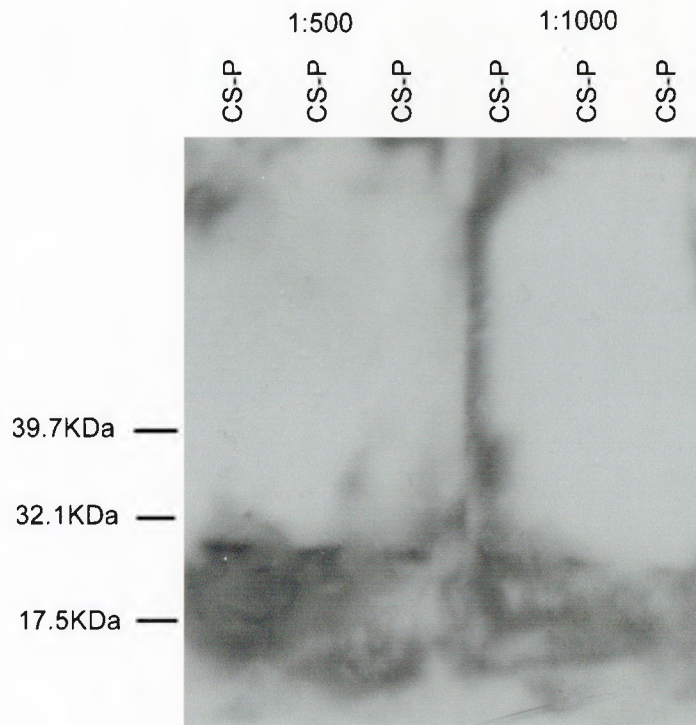
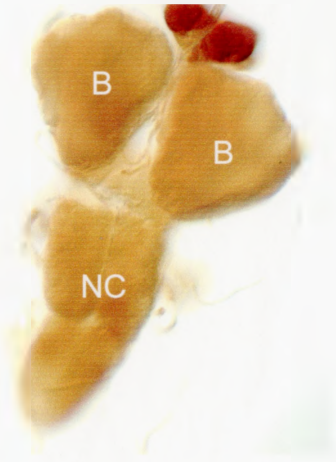


Figure 9. Immunostaining of CS-P larval CNS

Central nervous system of third instar larvae were dissected and stained with either the pre immune serum or the purified dVELI antibody. Antibody staining was found in the brain lobes (B) and the nerve cord (NC) as labeled with dVELI antibody.

pre immune



anti dveli



3.3 Misexpression of dVELI using UAS-GAL4 expression system

The UAS-GAL4 expression system is a target specific expression system that is adapted from the yeast transcription activation system. GAL4 is a yeast activator that controls the transcription of genes that are responsible for galactose metabolism. Each of these genes contains a GAL4 target site upstream of the transcription start site. These target sites are called Upstream Activating Sequences (UAS) (Weaver, 1999). Only when GAL4 binds to the Upstream Activation Sequence (UAS) of a certain gene, the transcription of that gene is activated.

This specifically controlled gene expression system is used in *Drosophila* studies. Many GAL4 lines were made that are used as the “driver” to drive gene expression in specific tissues or cell types. These constructs were made using the vectors containing the GAL4 coding sequence. For one type of the GAL4 constructs, promoters of some well characterized tissue specific genes are subcloned into these vectors at the sites upstream of the GAL4 sequence (Brand and Perrimon, 1993). Therefore, when the gene is expressed, GAL4 expression is also induced. Another type of GAL4 constructs used the enhancer detection vectors such as pGAWB. These vectors are P element transposons. Transcription of GAL4 is directed by the weak promoter of the P-transposase gene (Brand and Perrimon, 1993). The GAL4 coding sequence is randomly integrated into the fly genome upon the injection of the construct to the embryos. The gene expressions are controlled by the genomic enhancers, which are located near the sites of the insertions. When these GAL4 lines are crossed to the UAS lines (transgenic constructs that have a UAS sequence attached to the genes in study), the expression of the

gene of interest can be controlled. By using this UAS-GAL4 system, the expression of the gene in study can be directed to different tissue or cell types at different stages of development and hence the effects of the gene expression can be studied.

Effects of dVELI misexpression – viability tests

Three UAS-*dveli* constructs were made by Allison MacMullin (MacMullin, 2001): UAS-*lin7a*, UAS-*lin7b* and UAS-*lin7c*. All three constructs were mapped to be on the third chromosome as described in Appendix 3. These three UAS construct lines were tested with several neural or muscular GAL4 drivers such as *en* GAL4, *elav* GAL4, *sevenless* GAL4, *sim* GAL4, *ey* GAL4, *scab* GAL4, *pGMR* GAL4, *c179* GAL4, *twist* GAL4, *24B* GAL4 and *hs* GAL4. Embryo and larval viabilities of were tested. Figure 10 and 11 show the embryo and larval viabilities, respectively. There is no significant effect showed from these tests.

Figure 10. Embryo viability

Male and virgin female adult flies were collected and crossed from the three UAS-*lin7* construct and the GAL4 lines. Embryos from each cross were collected and tested for viability as described in method. The percentages in the table show the % of unhatched embryos from each cross after 48 hours incubation. The number in () shows the sample size.

	UAS lin7a	UAS lin7b	UAS lin7c	Parental GAL4
<i>24B</i>	38.7% (111)	29% (100)	11.2% (107)	39.6% (116)
<i>twist</i>	14.5% (583)	25% (526)	22.9% (501)	8.7% (537)
<i>C179</i>	16.3% (141)	24% (137)	27.9% (168)	11.1% (153)
<i>sim</i>	11.5% (104)	33% (106)	20% (40)	10.8% (101)
<i>Scab</i>	13.1% (235)	26.7% (209)	27.1% (214)	5.2% (211)
<i>pGMR</i>	14% (107)	1% (100)	2.9% (105)	5.6% (126)
<i>en</i>	9.9% (121)	12.9% (131)	29.8% (161)	35.3% (99)
<i>elav</i>	30.7% (387)	63.2% (500)	46.7% (293)	44% (404)
<i>sevenless/CyO</i>	50.7% (134)	58.1% (86)	24.3% (115)	21% (100)
<i>ey/CyO</i>	28.8% (218)	43.2% (238)	32.8% (189)	32.1% (196)
<i>hs/CyO</i>	23.7% (299)	30.3% (214)	39% (238)	40.6% (229)

Figure 11. Larval viability

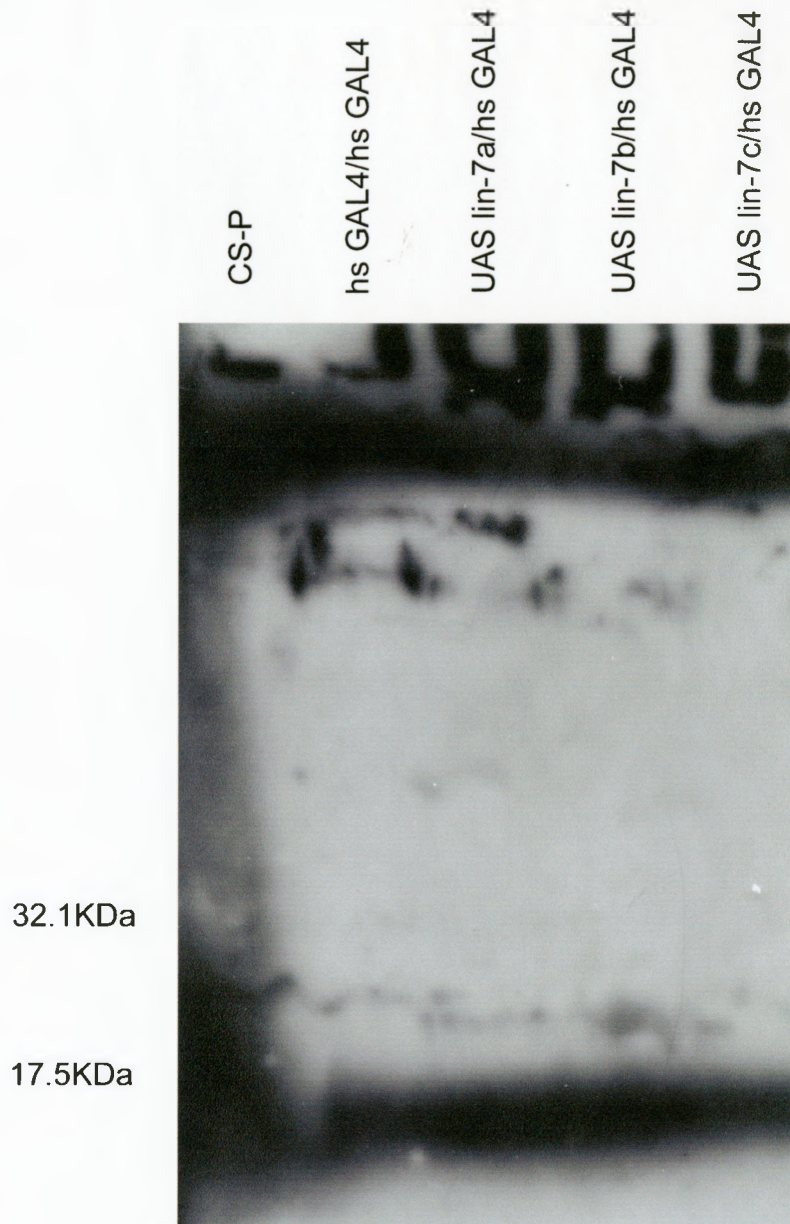
The hatched embryos from the embryo viability experiment were counted and transferred to glass tubes containing food medium, then the larval viability was calculated as described in method. This table shows the percentage of larvae develop to pupa stage and then adults. L→P indicate from larvae to pupae, P→A means from pupae to adults. The number in () is the sample size, the number in [] indicate the percentage of adults with curly wings. The upper table shows the viability test results when larvae were transferred at third instar stage, the lower one shows the results with the larvae transferred at first instar stage.

Western blot analysis for confirmation of protein expression

After the dVELI antibody was purified, the whole protein extracts of the heat-shocked UAS-*lin7s/hs GAL4* larvae were prepared and tested with Western blot analysis. The larvae were heat-shocked at 37°C for 45 minutes and then kept at room temperature for one hour for recovery before subjected to protein extraction. The method is adapted from heat-shock method described in Brand et al (Brand et al, 1994). Since *hs GAL4* should drive dVELI expression ubiquitously in the body tissues, the production of the protein should be at high level if the UAS constructs are working. Figure 12 shows the result of the Western blot. As indicated in the figure, the expression levels of dVELI are not differentiable from the wild type larvae (*CS-P*) to the UAS-*lin7/hs GAL4* larvae. Therefore, the results of this Western analysis show that the UAS constructs were not working, which explain why there are no significant effects showed in the viability experiments. Embryos from UAS-*lin7a/en GAL4* were stained with dVELI antibody as well, the expression pattern of *engrailed* was not observed in this test (data not shown). The result from embryo immunostaining also suggested that the UAS construct was not working.

Figure 12. Western blot analysis for confirmation of dVELI expression of the UAS-*lin7* constructs

Virgin female adult flies of UAS-*lin7s* and male adult flies of *hs GAL4* were collected and crossed. Third instar larvae of the progenies of these crosses, along with the larvae of *hs GAL4* were heat shocked at 37°C for 45 minutes and then were kept in room temperature for recovery and protein expression. After one-hour recovery, the larvae were collected for whole protein extraction as described in method. These protein samples along with the wild type (*CS-P*) larval protein sample were used for the Western blot analysis. The blot shows that the protein expression levels are not different among these samples, which shows dVELI expression was not directed by the *hs GAL4* driver.



3.4 RNA interference

RNA interference is a technique for interfering gene function. Double-stranded RNA (dsRNA) acts as a signal for silencing specific gene expression (Sharp, 1999). Its effect is specific for the gene it is derived from, and does not affect the expression of genes with unrelated sequences. *in situ* hybridization showed that dsRNA destabilize mRNA; the target mRNA concentration is reduced by as much as 90% (Tuschl et al, 1999). The molecular mechanism of RNA interference has been the focus of many researches. Recent studies showed that when dsRNA is introduced into the organisms or cells, it would be break down to small interfering RNA (siRNA) by an enzyme called Dicer. These siRNAs are then assembled into RNA-induced silencing complexes and are unwounded in the complexes. The complexes containing these siRNA strands then bind to the target mRNA. Upon the binding of siRNA with the complexes, the target mRNA is cleaved and degraded, hence the silencing of gene expression. Because of its profound effect on suppressing gene expression, RNAi is used in this thesis work to analyze *dveli* function.

Locomotion behavior effects upon RNA interference

There are different ways to deliver dsRNA to organisms or cell lines. The method used in this experiment is the soaking technique adapted from Dr. Davis' lab (Eaton et al, 2002) as described in method. Locomotion behavior of third instar larvae after introduction of dsRNA was tested. Since dVELI expression is localized at the neuromuscular junction, it is speculated that the locomotion behavior of the larvae would

be impaired by silencing the gene expression. Figure 13 shows the result of the behavior test. The behavior tests showed that larvae fed with double-stranded *dveli* RNA move slower than the control larvae (fed with buffer only). Other than the slower movement, there is no other phenotype being observed such as change in locomotion pattern. Many trials of the behavior test were done and variations were observed among different trials. The results of these tests are summarized in Appendix 6. Although there are variations, the general pattern is that larvae fed with *ds dveli* move slower than control ones.

Immunostaining of larval CNS to confirm silencing of gene expression by RNAi

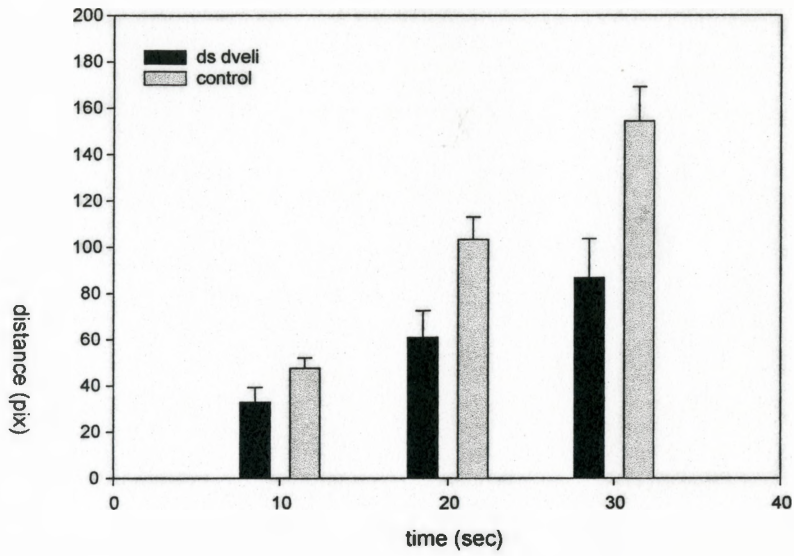
Since the locomotion behavior showed some effects that might be due to gene expression reduction, dVELI expression levels were tested by immunostaining. Central nervous system of third instar larvae that fed with *ds dveli*, *ds lacZ* and control were dissected and stained with anti-dVELI antibody. As illustrated in Figure 14, dVELI expression is reduced in the CNS of larvae fed with *ds dveli* but not in the CNS of larvae fed with *ds lacZ*. This result confirms the effectiveness and specificity of double-stranded *dveli*, also suggesting the slower movement phenotype is due to the dsRNA effect.

Figure 13. Locomotion behavior test result

For the result shown in test A, wild type (CS-P) late stage embryos were soaked in double-stranded *dveli* RNA (*ds dveli*) at the concentration of 900ng/ μ l. Controls are embryos soaked in RNAi buffer without dsRNA. Third instar larvae were tested for locomotion behavior in the dark for 30 seconds, the distances they moved were tracked and recorded at every ten seconds. The larvae tested in the trial were 13 for *ds dveli* and 16 for control. The p value for significance is 0.043 at 10 second, 0.013 at 20 seconds and 0.002 at 30 seconds. The p values were calculated using One-Way Analysis of Variance. For test B, larvae fed with *ds lacZ* were tested as well. Although there are variations within the individual larvae tested, the general pattern shows that larvae fed with *ds dveli* move slower than the ones fed with *ds lacZ* and buffer only.

A

Third instar larvae locomotion behavior test



B

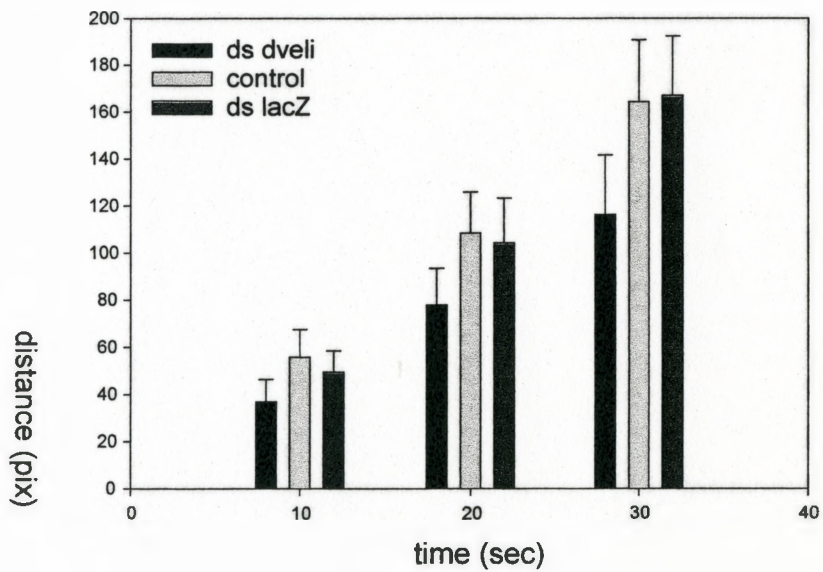
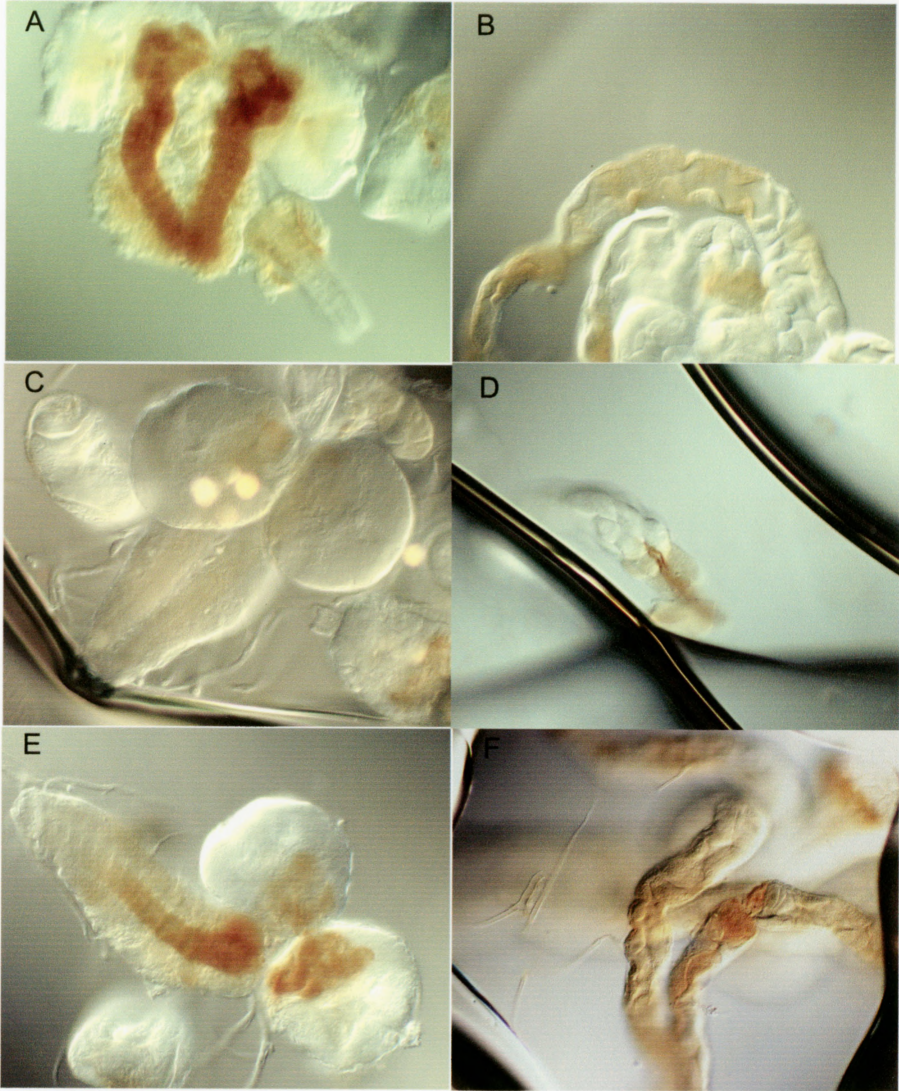


Figure 14. Immunostaining of larval CNS showing RNAi effect on gene expression

Panel A shows the brain of larvae from control (embryos soaked in RNAi buffer), it illustrated the expression pattern of dVELI. Panel C shows dVELI expression is profoundly reduced in the CNS of larvae fed with double-stranded *dveli* RNA (*ds dveli*). Panel E shows the CNS of larvae fed with double-stranded *lacZ* RNA. dVELI expression level is normal as in the control. Panel B, D, and F are the epithelial tissues from the control, *ds dveli* and *ds lacZ* larvae, respectively, showing the background staining levels are similar. Two trials of CNS immunostaining were tested. Totally 30 brains of the control larvae, 23 brains of *ds dveli* treated larvae and 21 brains of *ds lacZ* treated larvae were stained with dVELI antibody. There were variations of expression levels, but generally the expression of dVELI in *ds dveli* treated larvae were very low comparing to *ds lacZ* treated larvae and control ones.



Chapter 4

Discussion

Mutagenesis and functional analysis of *dveli* are the major objectives of this thesis work. P element insertional mutagenesis is the method used to generate mutants. Totally 138 potential mutant alleles were generated, however, the exact locations of the P element insertions have not been identified. A dVELI antibody was purified and tested for specificity. Western blot analysis and larval CNS immunostaining pattern indicate the specificity of this antibody. Misexpression of dVELI using UAS-GAL4 expression system at various tissues was done, but no significant results were observed. Further analysis suggested that the UAS constructs are invalid. RNAi experiments show that loss of *dveli* function results in slower locomotion behavior in *Drosophila* third instar larvae.

4.1 Generation and analysis of potential *dveli* mutants

One main focus of this thesis is to generate *dveli* mutants. P element mutagenesis is one of most extensively used methods, which does not involve any chemical or radioactive mutagenic agent. There are two types of P element constructs used in this mutagenesis method. One, the transposase, is within an immobile P element that encodes the 87 kDa transposase protein. The second type, the transposon construct, is stable in the genome unless transposase is provided. When flies containing a transposon are crossed to a transposase source, progeny will have a mobile P element within the germline, which may result in change of P element locations. P elements can cause

mutation by either insertion into genes or via imprecise excision from genes (Grigliatti, 1998). Insertion may disrupt gene function while excision causes deletion of a region.

The method used in this thesis work is the insertional mutagenesis method. The transposon line used has a P [lacW] construct inserted at the 5' end of the *OstStt3* gene, which is upstream of *dveli*. This transposon line was selected because it is close to *dveli* and it has been reported that *Drosophila* P elements preferentially move to genomic regions close to their original insertion sites (Tower et al, 1993). From our mutagenesis screen, about 14% of the tested lines were identified as having hopped out of the original P element insertion because they complemented the original P element line. Of these, 107 of the homozygously lethal lines and 31 of the non-lethal lines were identified to be on the third chromosome where *dveli* is.

A deficiency screen was done as mentioned in the Results section and Appendix 8. A control cross is done first to determine if the deficiency and the duplication are viable over the balancer chromosome *TM3*. The result shows that the ratio of the expected phenotypes of the progeny, normal body, non-*Sb*: normal body, *Sb*: black body, *Sb* is close to 3:1:1 rather than the estimated 2:1:1 ratio (Figure 6). The result suggests that *Df(3R)XTA1/TM3* and *Dp(3:3)M95A⁺13/TM3* are both viable but weak. The potential mutant alleles are crossed to the deficiency line. According to the results of the deficiency screen, 21 of the 107 homozygously lethal lines are likely to have lethal insertions near the chromosomal region of *dveli* (96B16) because they fail to complement the deficiency region by showing the progeny phenotypes ratio close to 1:1:1 (bold letters, Appendix 8). However, since the control cross does not show the expected ratio,

and some of these lethal lines show ratio values that are not close to the expected ones (*italic letters*, Appendix 8), the results of this deficiency screen are not definite. The difference in observed ratios may be due to different viability level caused by different P element insertion locations.

A PCR screen was done simultaneously to identify the exact location of the inserts. Three sets of primers were used to test the location of the P element (figure 7). Of the 138 potential alleles only 52 were tested due to time constraints (Table 1 shows the results). Nine of the 21 homozygously lethal lines that fail to complement the deficiency region according to the deficiency screen were subjected to this PCR screen (**bold letter**, Table 1). Four of them (E29, Q65, P6 and C62 in Table 1) showed results that were contradictory to the deficiency screen results as a fragment of 2.9kb was amplified by the P and 2 primer set, which suggested that the P elements are still located at the original insertion.

14 of those 52 tested lines should not have lethal insertions within the deficiency region according to the deficiency screen (*italic letter*, Table 1). However, 4 of them were shown by PCR to have insertions at the original P element location as P and 2 primers amplified fragments of 2.9 kb (K28, G18, P68 and N10 in Table 1). 22 of the 31 non-lethal lines were subjected to the PCR screen as well (right column, Table 1). Of them, 12 have inserts that located at the original P element insertion position as the P and 2 primer set amplified fragments about 2.9 kb long. The rest have P element inserts out of *OstStt3* but the exact locations are still unknown.

The PCR results contradict the results from complementation tests of the original P element insertion. One possible explanation for these results is that original P element insertion is not lethal, and there is another mutation in the genome causing the lethality. This possibility also explains the existence of the non-lethal lines with original P element insertions. The reason that these lines are non-lethal may be because the background mutation somehow reverted back to wild type. One possibility is that this background mutant is another P element insert and it was mobilized as well by the transposase to another location that does not cause lethality or it was excised out of the genome by the transposase. A plasmid rescue experiment can be done to test the possibility of the existence of the second P element. Plasmid rescue uses the characteristics of P element constructs, which contain an antibiotic-resistance gene (*amp^r* or *kan^r*) and restriction enzyme sites. When the genomic DNA is digested with the restriction enzymes, some of the fragments would contain part of the P element including the antibiotic-resistance gene and part of the flanking genomic DNA. These fragments are then treated by ligase to form small circular plasmid DNA, transformed into *E. coli*, and grown in medium containing the antibiotic. Only those containing the antibiotic-resistance gene would grow. The plasmid DNA is then purified and sequenced. The locations of the P elements can be determined by analyzing the sequence (Guo et al, 1996).

As the PCR screen is incomplete, no conclusion can be drawn from this mutagenesis experiment. No mutant allele of *dveli* has yet been identified. Further analysis of the locations of potential alleles is currently being carried on in Dr. Jacobs' lab by Dr. Firoz Mian. 12 tested lines have been identified to move toward *dveli* so far from Dr. Mian's

PCR screen results. Three of them are homozygously lethal lines and they are found to insert at about 3 kb upstream of 5' end of *dveli*. Nine of them are non-lethal lines and they all have P element insertions at 2.8 kb upstream of 5' end of *dveli*. Further analysis of these 12 potential alleles is an ongoing task to confirm the location of these insertions.

4.2 Analysis of dVELI antibody shows the specificity of this antibody

Rat serum containing dVELI antibody was generated by Allison MacMullin using a GST-dVELI fusion protein (MacMullin, 2001). Due to the loss of GST-dVELI construct and the affinity column required for antibody purification, a new protein construct was needed to generate a new affinity column. His-tagged dVELI was constructed. His tag was used instead of GST to avoid the cross-linking with the anti-GST antibody that may also exist in the serum. dVELI-His fusion protein was expressed and used to generate a new affinity column for dVELI antibody purification as described in Methods section.

An antibody of dVELI is important in determining the expression of the protein *in vivo* and *in vitro*. It also has biochemical importance as it can be used in a lot of biochemical interaction experiments such as co-immunoprecipitation for suspected binding partners. dVELI antibody was purified as described in the Methods and Results sections. To test the specificity of this antibody, a Western blot analysis was done using wild type adult fly whole protein extract. A band of approximately 24 kDa was detected as expected (Figure 8). The single band from the whole protein extract implies one *dveli* gene product in adult flies, unlike the three isoforms found in mammals. Immunostaining of larval CNS was further done to confirm the specificity of the antibody. dVELI

expression is concentrated in the brain lobes and neuropil area of the nerve cord as expected (MacMullin, 2001).

Western blot analysis and immunostaining results confirm the specificity of the purified antibody. They also further confirm the results shown in the previous report (MacMullin, 2001). dVELI staining pattern implies a neuronal function, especially in the synapse since it is concentrated in the neuropil area.

4.3 Misexpression of dVELI by the UAS-GAL4 system fail to show significant effects on viability, which may due to invalid UAS constructs

The UAS-GAL4 expression system is a very useful genetic tool for target specific expression. GAL4 was identified in the yeast *Saccharomyces cerevisiae* as an activator that regulates the expression of the genes responsible for galactose metabolism (Laughon et al 1984). Each of these genes contains a GAL4 target site called Upstream Activating Sequences (UAS). Only when GAL4 binds the UAS is transcription of that gene activated.

This specifically controlled gene expression system was then adapted in *Drosophila* studies. Many GAL4 constructs containing the *Gal4* coding region and a promoter sequence of a tissue specific gene are available. They are used as the “driver” to drive gene expression in the specific tissues or cell types controlled by the promoters. When these GAL4 lines are crossed to the UAS lines (transgenic constructs that have a UAS sequence attached to the genes in study), the expression of the gene of interest can be targeted to the specific tissue or cell types depending on the GAL4 constructs used. By

using this UAS-GAL4 system, the expression of the gene in study can be directed to different tissue or cell types at different stages of development and hence the effects of the gene expression can be studied.

Three UAS-*dveli* constructs were generated by Allison MacMullin (MacMullin, 2001), and they are named UAS-lin7a, UAS-lin7b and UAS-lin7c. The three UAS construct lines were tested with several neural and muscular GAL4 drivers, including *enGAL4*, *elavGAL4*, *sevenlessGAL4*, *simGAL4*, *eyGAL4*, *scabGAL4*, *pGMRGAL4*, *c179GAL4*, *twistGAL4*, *24BGAL4* and *hsGAL4*. Embryo and larval viabilities were tested as described in the results section (Figure 10 and 11). No significant effects were shown from these tests. Although some of the results show high percentage of embryonic lethality, for example in the case of expressing dVELI using *elav* GAL4 driver, the lethality is similar to the parental GAL4 stock control, which indicates that the lethality might due to the GAL4 construct and not the expression of dVELI. Of course, the expression of dVELI should be confirmed before any conclusion can be drawn.

To confirm the expression of dVELI from the UAS-lin7 constructs, whole protein extracts of the heat-shocked UAS-lin7/*hsGAL4* larvae were prepared and tested by Western blot analysis. Since *hsGAL4* should drive dVELI expression ubiquitously, the production of the protein should be at high levels if the UAS constructs are working. The heat-shock method used was adapted from the method described by Brand et al (Brand et al, 1994). The expression levels of dVELI do not differ from the wild type larvae (*CS-P*) and the parental *hsGAL4* stock (Figure 12). Therefore, the result of this Western blot analysis shows that dVELI expression is not driven by the *hsGAL4*, which further implies

that the UAS constructs are not working, and provides an explanation of why there are no significant effects shown in the viability experiments.

4.4 RNA interference tests indicate that *dveli* is involved in locomotion behavior

RNA interference (RNAi) is the general term for many posttranscriptional gene silencing (PTGS) phenomenon observed in many eukaryotic organisms including fungi, plants, nematodes and flies. It is induced by introducing double-stranded RNA (dsRNA) into the organism, which can trigger degradation of endogenous mRNAs that have the same sequence as the dsRNA. This effect was first demonstrated by Fire and colleagues using *C. elegans* as an experimental model organism (Fire et al, 1998). Since then, RNAi has been a powerful and widely used genetic tool for silencing gene function.

The mechanism of RNAi has been the focus of intense studies for the past few years as more and more molecules that are involved in RNAi have been discovered. Different mechanistic models of RNAi have been proposed for different organisms. A common feature of RNAi is the presence of 21-25 nucleotide dsRNAs called small interference RNAs (siRNAs). It is believed that upon the introduction of dsRNA to the organism, it is cleaved into siRNAs, which will later trigger the gene silencing effects. The observation of siRNA led to the discovery of Dicer, a member of RNase III family, which are dsRNA-specific nucleases (Bernstein et al, 2001). Dicer was first identified in *Drosophila* with homologs from other organisms later being identified. The initial RNAi cleavage step into siRNAs is performed by Dicer.

One of the RNAi pathway models suggested that siRNAs act as guides for RNA-binding proteins that are responsible for degradation of the target mRNA (Schwarz et al, 2002). In this pathway model, the siRNAs are first bound by RNA-binding proteins to form the ribonucleoprotein complex RISC (RNA-induced silencing complex). When siRNAs are activated by ATP, they are unwound and will guide the activated RISC complex to the target mRNA, cleave it, and silence the expression of the gene.

RNAi has been adapted as a reverse genetic tool to study gene function in *Drosophila*. There are different methods used to deliver the synthesized dsRNA into the organism. Microinjection is the most commonly method used. In *C. elegans*, it was shown that the site of injection is not critical, suggesting that dsRNAs may be transported into cells from wherever it is injected (Fire et al, 1998). The method used in this thesis work is adapted from a study reported by Dr. Davis' lab (Eaton et al, 2002). Instead of injecting dsRNA to the embryos, late stage embryos were soaked in RNAi solutions containing synthesized dsRNA (detail description in Methods).

Wild type (CS-P) late stage embryos were soaked in ds *dveli*, ds *LacZ*, or buffer only. Locomotion behavior was tested after they developed to third instar larvae. Several trials of behavior tests were done as summarized in Appendix 6. There are variations among the tests and also variations were found among individual larvae from the same soaking batch. Although variations exist, the general pattern is that larvae fed with ds *dveli* move slower than the ones fed with either ds *lacZ* or buffer only. Because dVELI is localized at the postsynaptic area in larval NMJ, it is speculated to have synaptic function. RNAi effects suggest it may function in synaptic signal transduction. One possible function of

dVELI may be in proper localization of neurotransmitter receptors in the postsynaptic area.

CNS of the tested larvae were dissected and stained with dVELI antibody. The immunostaining showed that dsRNA of *dveli* does reduce the protein production (Figure 14). The immunostaining results showed the efficacy of this technique and suggest the behavior phenotype is possibly due to the silencing of *dveli* expression. Also, the staining of ds *lacZ* treated larval CNS show the RNAi effect is specific. However, analysis of the NMJ of ds *dveli* treated larvae should be done to further elucidate the effect of RNAi on the loss of *dveli* function in NMJ. For example, staining the NMJ with known pre- and postsynaptic proteins might show disruption of the structure if dVELI is required for NMJ formation or stabilization. Also, staining the NMJ with known neurotransmitter receptors such as DGluRIIA and DGluRIIB might show mislocalization of these receptors if dVELI is required for proper localization of the receptors.

Studies of mammalian homologs have linked Velis to the NMDA glutamate receptor subunit NR2B (Jo et al, 1999). Since dVELI shares high homology to Velis, it might also interact with neurotransmitter receptors in the postsynaptic membrane. Three candidates in *Drosophila* are the *Drosophila* glutamate receptor IIA (DGluRIIA), DGluRIIB, and a recently identified DGluRIII. All three receptors are expressed in muscle at the neuromuscular junction. DGluRIIA and DGluRIIB have redundant function and neither is required for viability (DiAntonio et al, 1999). A recent study identified a new glutamate receptor subunit, DGluRIII, which is essential for viability and the localization of DGluRIIA and DGluRIIB (Marrus et al, 2004). This novel receptor subunit exhibits a

class II C-terminal PDZ-binding motif, suggesting it may interact with a PDZ domain containing protein, possibly dVELI as this class II PDZ interaction corresponds to mammalian VELI binding to NR2B subunit of NMDA receptor.

4.5 Potential formation of CMG/dVELI/dX11L complex and its function

Orthologs of *lin-2/Cask*, *lin-7/velis*, and *lin-10/Mints* have been identified in *Drosophila*, namely *camguk (cmg)/caki*, *dveli*, and *dX11L*, respectively (Martein and Ollo, 1996; MacMullin, 2001; Hase et al, 2002). Since these orthologs show homology to their *C. elegans* and mammalian counterparts, it is speculated that a tripartite protein complex, CMG/dVELI/dX11L, also exists in *Drosophila*. *Camguk/caki* is highly expressed in the central nervous system throughout the developmental stages (Martin and Ollo, 1996). *dveli* was found in the larval and adult CNS as well (MacMullin, 2001). *dX11L* has been reported to express in neuronal tissues from middle stage of embryo to adult (Hase et al, 2002). As expression patterns of these genes are similar to their mammalian orthologs, these genes may have a similar function as their mammalian counterparts.

Although the *Drosophila* orthologs of these three genes have been identified, their functions are still unclear. Also, the formation of the tripartite protein complex has not been confirmed. *Camguk/Caki* has been reported to be involved in behavior change. A study reported that *caki*¹ mutant flies showed reduced walking speed (Martin and Ollo, 1996). Our results also show that loss of *dveli* function causes slower larval movement. These results imply that CMG and dVELI might function together in the synapse, either

for proper localization of neurotransmitter receptors or for synaptic junction formation, as in mammals. To prove this hypothesis, the temporal and spatial interaction of CMG and dVELI has to be elucidated. Also, further examination of behavior changes in *camguk* mutant larvae and *dveli* mutant adults is required.

In *C. elegans* and mammals, LIN-10/Mint participates in this tripartite complex through the interactions with LIN-2/CASK (Kaech et al, 1998; Butz et al, 1998). This interaction has not been identified in the known *Drosophila* homologs. One important thing to note is the identified dX11L is similar to the mammalian Mint 2. However, in the three known mammalian Mints, Mint 1 is the only one that has been identified to interact with CASK (Okamoto and Sudhof, 1997). Of course the possible interaction between CAMGUK and dX11L cannot be ruled out, however, it is possible that more than one *Drosophila* LIN-10 exists and each may be involved in a different protein complex. Further analysis of the genome may reveal other *dlin-10s* and their potential interaction with *dveli*.

Mammalian homologs of dVELI have been implicated in a variety of interactions. Other than binding to Cask, Velis also bind to PALS-1 through the L27 domain. *Drosophila* homolog of PALS-1, Stardust (Sdt), has been identified. Sdt is involved in cell polarity establishment and maintenance (Bachmann et al, 2001). It is possible that dVELI also interacts with Sdt and has a role in cell polarity. Since *dveli* was first identified to interact with *Drosophila Egfr (DER)*, it suggests that *dveli* has epithelial function as well. dVELI may be involved in the localization of DER, similar to the function of its *C. elegans* homolog. A recent study also revealed the interaction between

mammalian Lin-7 and the EGFR like receptor, ErbB-2 (Shelly et al, 2003). In their study, a new protein interacting domain, KID, was found in human Lin-7b. KID domain is responsible for the basolateral membrane localization of ErbB-2, while the PDZ domain is important for the retention of the receptor at the basolateral membrane. This newly identified KID domain is conserved in evolution (Shelly et al, 2003). A BLAST search using amino acid residues 7-28 (the KID domain) of human Lin-b protein sequence (NCBI accession # NM_022165) did not pull out similar sequence from *Drosophila* database. However, when comparing the dVELI sequence to the whole protein sequence of hLin-7b, it shows a 53% identity with the KID domain amino acid sequence, which suggests that a KID domain may exist in dVELI as well. Further analysis of the sequence and biochemical interaction experiments will reveal the identity and importance of this motif in dVELI.

Mammalian LIN-7 has also been linked to beta-catenin (Perego et al, 2000, Bamji et al, 2003). The epithelial and neuronal junctional domains are composed of cell adhesion molecules (CAM) for proper cell-cell adhesion. One major type of these CAMs is the Ca²⁺-dependent cadherins. These transmembrane proteins interact with catenins through their cytoplasmic regions. Catenins mediate the connections of cadherins to the actin cytoskeleton, which strengthens the cell-cell adhesion. It will be interesting to know if dVELI also interact with *Drosophila* catenins. This finding will further confirm the possible role of dVELI in cell-cell adhesion.

4.6 Direction of future research

Mammalian homologs of dVELI have been implicated in a variety of processes, such as cell-cell adhesion (Perego et al, 2000; Yamamoto et al, 2002), neurotransmitter receptor localization (Jo et al, 1999), ion channels localization (Olsen et al, 2002), epithelial growth factor receptor targeting (Shelly et al, 2003) and cell polarity (Roh et al, 2002). By homology, it is implied that dVELI may have similar functions in different cell types. To test the possible roles of dVELI, the interactions of dVELI with other protein should be identified. A yeast two hybrid assay using *dveli* as bait and an adult *Drosophila* cDNA library is currently being conducted in Dr. Jacobs' lab to test possible interactions. Hopefully the finding of more dVELI interacting partners will lead to more understanding of its function.

Determination of potential mutants from the P element insertional mutagenesis is also an ongoing task. Any insertion that moved closer to or right in *dveli* may cause a mutant phenotype and can be used to study *dveli* function. Also, insertions that are close to *dveli* but do not affect gene function can be used for further mutagenesis such as imprecise excision, which may delete part of, or the whole *dveli* region, and hence cause loss of function mutants.

The primary RNAi experiment showed that dVELI is required for locomotion speed. How it affects locomotion behavior is still unknown. Analysis of the ultrastructure of NMJ should present a clearer understanding. An ongoing experiment in Dr. Jacobs' lab is to design a heritable and inducible RNAi construct: the UAS *dveli* hairpin construct. By using this construct, *dveli* dsRNA can be expressed *in vivo*, and the expression can be

targeted at different tissue types using the UAS-GAL4 expression system. The advantages of this construct include economic benefits and eliminating the difficulty of delivering synthesized dsRNA to the organism. By targeting gene silencing using the UAS-GAL4 system, the role of *dveli* at different tissue types may be elucidated.

Our primary results show that dVELI is involved in larval locomotion behavior, as well as a possible role in synapse formation and/or neurotransmitter signaling. It is hoped the ongoing experiments will provide further information on the role of dVELI in the synapse as well as the identification of novel functions.

Reference

Bachmann, A., Schneider, M., Theilenberg, E., Grawe, F., and Knust, E. 2001. *Drosophila* Stardust is a partner of Crumbs in the control of epithelial cell polarity. *Nature*. 414: 638-643

Bamji, S. X., Shimazu, K., Kimes, N., Huelsken, J., Birchmeier, W., Lu, B., and Reichardt, L. 2003. Role of beta-catenin in synaptic vesicle localization and presynaptic assembly. *Neuron*. 40: 719-731

Bernstein, E., Caudy, A. A., Hammond, S. M., and Hannon, G. J. 2001. Role for a bidentate ribonuclease in the initiation step of RNA interference. *Nature*. 409: 363-366

Biederer, T., Cao, X., Sudhof, T. C., and Liu, X. 2002. Regulation of APP-dependent transcription complexes by Mint/X11s: differential functions of Mint isoforms. *J Neuroscience*. 22: 7340-7351

Bilder, D. and Perrimon, N. 2000. Localization of apical epithelial determinants by the basolateral PDZ protein Scribble. *Nature*. 403: 676-680

Bilder, D. 2001. PDZ proteins and polarization: functions from the fly. *Trends in Genetics*. 17: 511-519

Bilder, D., Schober, M., and Perrimon, N. 2003. Integrated activity of PDZ protein complexes regulates epithelial polarity. *Nature Cell Biology*. 5: 53-58

Brand, A. H., Manoukian, A. S., and Perrimon, N. 1994. Ectopic Expression in *Drosophila* in Goldstein, L. S. B. and Fyrberg, E. A., ed. *Methods in Cell Biology Volume 44: Drosophila melanogaster: practical uses in cell and molecular biology*. Academic Press. Pp635-654

Brenman, J. E., Chao, D. S., Gee, S. H., McGee, A. W., Craven, S. E., Santillano, D. R., Wu, Z., Huang, F., Xia, H., Peters, M. F., Froehner, S. C., and Brecht, D. S. 1996. Interaction of nitric oxide synthase with the postsynaptic density protein PSD-95 and alpha1-syntrophin mediated by PDZ domains. *Cell*. 84: 757-67

Butz, S., Okamoto, M., and Sudhof, T. C. 1998. A tripartite protein complex with the potential to couple synaptic vesicle exocytosis to cell adhesion in brain. *Cell*. 94: 773-782

Cohen, A. R., Woods, D. F., Marfatia, S. M., Walther, Z., Chishti, A. H., Anderson, J. M., and Woods, D. F. 1998. Human CASK/LIN-2 binds syndecan-2 and protein 4.1 and localizes to the basolateral membrane of epithelial cells. *J Cell Biol*. 142:129-138

Cuppen, E., Gerrits, H., Pepers, B., Wieringa, B., and Hendriks, W. 1998. PDZ motifs in PTP-BL and RIL bind to internal protein segments in the LIM domain protein RIL. *Mol Biol Cell*. 9: 671-83

Dawkins, R., and Dawkins, M. 1976 Hierarchical organization and postural facilitation: rules for grooming in flies. *Anim. Behav.* 24: 739-755

DiAntonio, A., Petersen, S. A., Heckmann, M., and Goodman, C. S. 1999. Glutamate receptor expression regulates quantal size and quantal content at the *Drosophila* neuromuscular junction. *J Neurosci*. 19: 3023-3032

Dimitratos, S. D., Woods, D. F., and Bryant, P. J. 1997. Camguk, Lin-2 and CASK: novel membrane-associated guanylate kinase homologs that also contain CaM kinase domains. *Mech. Dev.* 63: 127-130

Doerks, T., Bork, P., Kamberov, E., Makarova, O., Muecke, S., and Margolis, B. 2000. L27, a novel heterodimerization domain in receptor targeting proteins Lin-2 and Lin-7. *Trends Biochem Sci*. 25:317-8

Dong, H., Zhang, P., Song, I., Petralia, R. S., Liao, D., and Huganir, R. L. 1999. Characterization of the glutamate receptor-interacting proteins GRIP1 and GRIP2. *J Neurosci*. 19: 6930-6941

Doyle, D. A., Lee, A., Lewis, J., Kim, E., Sheng, M., and MacKinnon, R. 1996. Crystal structures of a complexed and peptide-free membrane protein-binding domain: molecular basis of peptide recognition by PDZ. *Cell*. 85:1067-1076

Eaton, B. A., Fetter, R. D., and Davis, G. W. 2002. Dynactin is necessary for synapse stabilization. *Neuron*. 34: 729-741

Eisenmann, D. M. and Kim, S. K. 1994. Signal transduction and cell fate specification during *Caenorhabditis elegans* vulval development. *Curr. Opin. in Genet. Develop.* 4: 508-516

Fallon, L., Moreau, F., Croft, B. G., Labib, N., Gu, W., and Fon, E. A. 2002. Parkin and CASK/LIN-2 associate via a PDZ-mediated interaction and are co-localized in lipid rafts and postsynaptic densities in brain. *J Biol. Chem.* 277: 486-491

Fire, A., Xu, S. Q., Montgomery, M. K., Kostas, S. A., Driver, S. E., and Mello, C. C. 1998. Potent and specific genetic interference by double-stranded RNA in *Caenorhabditis elegans*. *Nature*. 391: 806-811

FlyBase. 2004. <http://flybase.bio.indiana.edu/>

Garner, C. C., Nash, J., and Huganir, R. L. 2000. PDZ domains in synapse assembly and signaling. *Trends in Cell Biology*. 10: 274-280

Giot, L., Bader, J. S., Brouwer, C., Chaudhuri, A., Kuang, B., Li, Y., Hao, Y. L., Ooi, C. E., Godwin, B., Vitols, E., Vijayadamodar, G., Pochart, P., Machineni, H., Welsh, M., Kong, Y., Zerhusen, B., Malcolm, R., Varrone, Z., Collis, A., Minto, M., Burgess, S., McDaniel, L., Stimpson, E., Spriggs, F., Williams, J., Neurath, K., Ioime, N., Agee, M., Voss, E., Furtak, K., Renzulli, R., Aanensen, N., Carrolla, S., Bickelhaupt, E., Lazovatsky, Y., DaSilva, A., Zhong, J., Stanyon, C. A., Finley, R. L. Jr, White, K. P., Braverman, M., Jarvie, T., Gold, S., Leach, M., Knight, J., Shimkets, R. A., McKenna, M. P., Chant, J., and Rothberg, J. M. 2003. A protein interaction map of *Drosophila melanogaster*. *Science*. 302: 1727-1736

Grigliatti, T. A. 1998. Transposons-gene tagging and mutagenesis in Roberts, D. B., ed. *Drosophila* second ed. Oxford: Oxford University Press pp85-107

Grootjans, J.J., Reekmans, G., Ceulemans, H., and David, G. 2000. Syntenin-syndecan binding requires syndecan-synteny and the co-operation of both PDZ domains of syntenin. *J Biol Chem*. 275: 19933-41

Gonzalez-Mariscal, L., Betanzos, A., and Avila-Flores, A. 2000. MAGUK proteins: structure and role in the tight junction. *Cell and Developmental Biology*. 11: 315-324

Harris, B. Z., Venkatasubrahmanyam, S., and Lim, W. A. 2002. Coordinated folding and association of the LIN-2, -7 (L27) domain. *J Biol Chem*. 277: 34902-34908

Hase, M., Yagi, Y., Taru, H., Tomita, S., Sumioka, A., Hori, K., Miyamoto, K., Sasamura, T., Nakamura, M., Matsuno, K., and Suzuki, T. 2002. Expression and characterization of the *Drosophila* X11-like/Mint protein during neural development. *J Neurochem*. 81: 1223-32

Hata, Y., Butz, S., and Sudhof, T. C. 1996. CASK: a novel dlg/PSD95 homolog with an N-terminal calmodulin-dependent protein kinase domain identified by interaction with neuexins. *J Neurosci*. 16: 2488-94

Hata, Y., Nakanishi, H., and Takai, Y. 1998. Synaptic PDZ domain-containing proteins. *Neuroscience Research*. 32: 1-7

Hsueh, Y. P., Kim, E., and Sheng, M. 1997. Disulfide-linked head-to-head multimerization in the mechanism of ion channel clustering by PSD-95. *Neuron*. 18: 803-814

Hsueh, Y. P., Yang, F. C., Kharazia, V., Naisbitt, S., Cohen, A. R., Weinberg, R. J., and Sheng, M. 1998. Direct interaction of CASK/LIN-2 and syndecan heparan sulfate proteoglycan and their overlapping distribution in neuronal synapses. *J Cell Biol.* 142: 139-151

Hung, A. Y., and Sheng, M. 2002. PDZ domains: structural modules for protein complex assembly. *J. of Biol. Chem.* 277: 5699-5702

Irie, M., Hata, Y., Takeuchi, M., Ichtchenko, K., Toyoda, A., Hirao, K., Takai, Y., Rosahl, T. W., and Sudhof, T. C. 1997. Binding of neuroligins to PSD-95. *Science.* 277: 1511-1515

Iyengar, B. G. 2002. Development of larval photobehaviour as a paradigm to identify mutations that affect nervous system development and function. PhD thesis. McMaster University.

Jo, K., Derin, R., Li, M., and Brecht, D. S. 1999. Characterization of MALS/Velis-1, -2, and -3: a family of mammalian LIN-7 homologs enriched at brain synapses in association with the Postsynaptic Density-95/NMDA receptor postsynaptic complex. *J Neuroscience.* 19: 4189-4199

Kaech, S. M., Whitfield, C. W., and Kim, S. K. 1998. The LIN-2/LIN-7/LIN-10 complex mediates basolateral membrane localization of the *C. elegans* EGF receptor LET-23 in vulval epithelial cells. *Cell.* 94: 761-771

Kamberov, E., Makarova, O., Roh, M., Liu, A., Karnak, D., Straight, S., and Margolis, B. 2000. Molecular cloning and characterization of Pals, proteins associated with mLin-7. *J Biol Chem.* 275: 11425-11431

Kim, E., Niethammer, M., Rothschild, A., Jan, Y. N., and Sheng, M. 1995. Clustering of Shaker-type K⁺ channels by interaction with a family of membrane-associated guanylate kinases. *Nature.* 378: 85-8

Koh, Y. H., Gramates, L. S., and Budnik, V. 2000. *Drosophila* larval neuromuscular junction: molecular components and mechanisms underlying synaptic plasticity. *Microscopy Research and Technique.* 49: 14-25.

Kornau, H. C., Schenker, L. T., Kennedy, M. B., and Seeburg, P. H. 1995. Domain interaction between NMDA receptor subunits and the postsynaptic density protein PSD-95. *Science.* 269: 1737-40

Laughon, A., Driscoll, R., Wills, N., and Gesteland, R. F. 1984. Identification of two proteins encoded by the *Saccharomyces cerevisiae* GAL4 gene. *Mol Cell Biol* 4: 268-275

Lopes C., Gassanova, S., Delabar, J., and Rachidi, M. 2001. The CASK/Lin-2 *Drosophila* homologue, *Camguk*, could play a role in epithelial patterning and in neuronal targeting. *Biochemical and Biophysical Research Communications*. 284: 1004-1010

MacMullin, A. A. 2001. Identification and molecular characterization of *dveli*, the *Drosophila* ortholog of *C. elegans* *lin-7*. Master thesis. McMaster University

Marrus, S. B., Portman, S. L., Allen, M. J., Moffat, K. G., and DiAntonio, A. 2004. Differential localization of glutamate receptor subunits at the *Drosophila* neuromuscular junction. *J Neurosci*. 24: 1406-1415

Martin, J. R. and Ollo, R. 1996. A new *Drosophila* Ca²⁺/calmodulin-dependent protein kinase (Caki) is localized in the central nervous system and implicated in walking speed. *EMBO J*. 15: 1865-1876

Mathew, D., Gramates, L. S., Packard, M., Thomas, U., Bilder, D., Perimon, N., Gorczyca, M., and Budnik, V. 2002. Recruitment of Scribble to the synaptic scaffolding complex requires GUK-holder, a novel Dlg binding protein. *Current Biology*. 12: 531-539

Mendoza, C., Olguin, P., Lafferte, G., Thomas, U., Ebitsch, S., Gundelfinger, E. D., Kukuljan, M., and Sierralta, J. 2003. Novel isoforms of Dlg are fundamental for neuronal development in *Drosophila*. *J. of Neuroscience*. 23: 2093-2101

Muller, H. J. 2000. Genetic control of epithelial cell polarity: lessons from *Drosophila*. *Developmental Dynamics*. 218: 52-67

Morais Cabral, J. H., Petosa, C., Sutcliffe, M. J., Raza, S., Byron, O., Poy, F., Marfatia, S. M., Chishti, A. H., and Liddington, R. C. 1996. Crystal structure of a PDZ domain. *Nature*. 382: 649-652

O'Hare, K. and Rubin, G. M. 1983. Structures of P transposable elements and their sites of insertion and excision in the *Drosophila melanogaster* genome. *Cell*. 34: 25-35

Ohshiro, T., Yagami, T., Zhang, C., and Matsuzaki, F. 2000. Role of cortical tumour-suppressor proteins in asymmetric division of *Drosophila* neuroblast. *Nature*. 408: 593-596

Okamoto, M. and Sudhof, T. C. 1997. Mints, Munc18-interacting proteins in synaptic vesicle exocytosis. *J Biol. Chem*. 272: 31459-31464

- Okamoto, M. and Sudhof, T. C. 1998. Mint 3: a ubiquitous mint isoform that does not bind to munc18-1 or -2. *Eur. J Cell Biol.* 77: 161-165
- Olsen, O., Liu, H., Wade, J. B., Merot, J., and Welling, P. A. 2002. Basolateral membrane expression of the Kir 2.3 channel is coordinated by PDZ interaction with Lin-7/CASK complex. *Am J Physiol Cell Physiol.* 282: C183-C195
- Packard, M., Mathew, D., and Budnik, V. 2003. FAST remodeling of synapses in *Drosophila*. *Curr. Opin. In Neurobiol.* 13: 527-534
- Perego, C., Vanoni, C., Villa, A., Longhi, R., Kaech, S. M., Frohli, E., Hajnal, A., Kim, S. K., and Pietrini, G. 1999. PDZ-mediated interactions retain the epithelial GABA transporter on the basolateral surface of polarized epithelial cells. *The EMBO Journal.* 18: 2384-2393
- Perego, C., Vanoni, C., Massari, S., Longhi, R., and Pietrini, G. 2000. Mammalian LIN-7 PDZ proteins associate with β -catenin at the cell-cell junctions of epithelia and neurons. *The EMBO Journal.* 19: 3978-3989
- Phillis, R. W., Bramlage, A. T., Wotus, C., Whittaker, A., Gramates, L. S., Seppala, D., Farahanchi, F., Caruccio, P., and Murphey, R. K. 1993. Isolation of mutations affecting neural circuitry required for grooming behavior in *Drosophila melanogaster*. *Genetics.* 133: 581-592
- Pielage, J., Stork, T., Bunse, I., and Klambt, C. 2003. The *Drosophila* cell survival gene *discs lost* encodes a cytoplasmic Codanin-1-like protein, not a homolog of tight junction PDZ protein Patj. *Developmental Cell.* 5: 841-851
- Ponting, C. P. 1997. Evidence for PDZ domains in bacteria, yeast, and plants. *Protein Science.* 6: 464-468
- Rio, D. C., Laski, F. A., and Rubin, G. M. 1986. Identification and immunochemical analysis of biologically active *Drosophila* P element transposase. *Cell.* 44: 21-32
- Roche, J. P., Packard, M. C., Moeckel-Cole, S., and Budnik, V. 2002. Regulation of synaptic plasticity and synaptic vesicle dynamics by the PDZ protein Scribble. *J. of Neuroscience.* 22: 6471-6479
- Roh, M. H., Makarova, O., Liu, C. J., Shin, K. Y., Lee, S., Laurinec, S., Goyal, M., Wiggins, R., and Margolis, B. 2002. The Maguk protein, Pals1, functions as an adapter, linking mammalian homologues of Crumbs and Discs Lost. *J. of Cell Biol.* 157: 161-172

- Roh, M. H., Fan, S., Liu, C. J., and Margolis, B. 2003. The Crumbs3-Pals1 complex participates in the establishment of polarity in mammalian epithelial cells. *J. of Cell Science*. 116: 2895-2906
- Roh, M. H. and Margolis, B. 2003. Composition and function of PDZ protein complexes during cell polarization. *Am. J. Physiol. Renal. Physiol.* 285: F377-F387
- Setou, M., Nakagawa, T., Seog, D. H., and Hirokawa, N. 2000. Kinesin superfamily motor protein KIF17 and mLin-10 in NMDA receptor-containing vesicle transport. *Science*. 288: 1796-1802
- Rongo, C., Whitfield, C. W., Rodal, A., Kim, S. K., and Kaplan, J. M. 1998. LIN-10 is a shared component of the polarized protein localization pathways in neurons and epithelia. *Cell*. 94: 751-759
- Rubin, G. M., Kidwell, M. G., and Bingham, P. M. 1982. The molecular basis of P-M hybrid dysgenesis: the nature of induced mutations. *Cell*. 29: 987-994
- Schultz, J., Copley, R. R., Doerks, T., Ponting, C.P., and Bork, P. 2000. SMART: a web-based tool for the study of genetically mobile domains. *Nucleic Acids Res.* 28: 231-234.
- Schuster, C. M., Davis, G. W., Fetter, R. D., and Goodman, C. S. 1996. Genetic dissection of structural and functional components of synaptic plasticity. I. Fasciclin II controls synaptic stabilization and growth. *Neuron*. 17: 641-654
- Schwarz, D. S., Hutvagner, G., Haley, B., and Zamore, P. D. 2002. Evidence that siRNAs function as guides, not primers, in the *Drosophila* and human RNAi pathways. *Mol Cell*. 10: 537-548
- Shelly, M., Mosesson, Y., Citri, A., Lavi, S., Zwang, Y., Melamed-Book, N., Aroeti, B., and Yarden, Y. 2003. Polar expression of ErbB-2/HER2 in epithelia: bimodal regulation by Lin-7. *Developmental Cell*. 5: 475-486
- Sheng, M. and Sala, C. 2001. PDZ domain and the organization of supramolecular complexes. *Annu. Rev. Neurosci.* 24: 1-29
- Simske, J. S., Kaech, S. M., Harp, S. A., and Kim, S. K. 1996. LET-23 receptor localization by the cell junction protein LIN-7 during *C. elegans* vulval induction. *Cell*. 85: 195-204
- Songyang, Z., Fanning, A. S., Fu, C., Xu, J., Marfatia, S. M., Chishti, A. H., Crompton, A., Chan, A. C., Anderson, J.M., and Cantley, L.C. 1997. Recognition of unique carboxyl-terminal motifs by distinct PDZ domains. *Science*. 275:73-77

Stricker, N. L., Christopherson, K. S., Yi, B. A., Schatz, P. J., Raab, R. W., Dawes, G., Bassett, D. E. Jr, Bredt, D. S., and Li, M. 1997. PDZ domain of neuronal nitric oxide synthase recognizes novel C-terminal peptide sequences. *Nat Biotechnol.* 15: 336-342

Tanentzapf, G. and Tepass, U. 2002. Interactions between the *crumbs*, *lethal giant larvae* and *bazooka* pathways in epithelial polarization. *Nature Cell Biology.* 5: 46-52

Tejedor, F. J., Bokhari, A., Rogero, O., Gorczyca, M., Zhang, J., Kim, E., Sheng, M., and Budnik, V. 1997. Essential role for *dlg* in synaptic clustering of Shaker K⁺ channels *in vivo*. *J Neuroscience.* 17: 152-159

Tepass, U., Theres, C., and Knust, E. 1990. *crumbs* encodes an EGF-like protein expressed on apical membranes of *Drosophila* epithelial cells and required for organization of epithelia. *Cell.* 6: 787-799

Tepass, U., Tanentzapf, G., Ward, R. and Fehon, R. 2001. Epithelial cell polarity and cell junctions in *Drosophila*. *Annu. Rev. Genet.* 35: 747-784

Thomas, U., Kim, E., Kuhlendahl, S., Koh, Y. H., Gundelfinger, E. D., Sheng, M., Garner, C. C., and Budnik V. 1997. Synaptic clustering of the cell adhesion molecule fasciilin II by discs-large and its role in the regulation of presynaptic structure. *Neuron.* 19: 787-799

Tower, J., Karpen, G. H., Craig, N., and Spradling, A. C. 1993. Preferential transposition of *Drosophila* P elements to nearby chromosomal sites. *Genetics.* 133: 347-359

Tseng, T. C., Marfatia, S. M., Bryant, P. J., Pack, S., Zhuang, Z., O'Brien, J. E., Lin, L., Hanada, T., and Chishti, A. H. 2001. VAM-1: a new member of the MAGUK family binds to human Veli-1 through a conserved domain. *Biochim Biophys Acta.* 1518: 249-59

Yamamoto, Y., Mandai, K., Okabe, N., Hoshino, T., Nakanishi, H., and Takai, Y. 2002. Localization of mLin-7 at nectin-based cell-cell junctions. *Oncogene.* 21: 2545-2554.

Zhang, M. and Wang, W. 2003. Organization of signaling complexes by PDZ-Domain Scaffold Proteins. *Acc. Chem. Res.* 36: 530-538.

List of Appendices

Appendix 1	Adult fly grooming behavior assay	104
Appendix 2	Time required for adult flies to recover from CO ₂ treatment	107
Appendix 3	Genetic scheme for mapping the chromosomal location of UAS-lin7s	109
Appendix 4	pET29b+ multiple cloning sites	111
Appendix 5	LITMUS 28i multiple cloning sites	113
Appendix 6	Locomotion behavior test of dsRNA treated larvae	115
Appendix 7	beta-galactosidase activity assay for ds lacZ efficiency	117
Appendix 8	Deficiency screen results	120

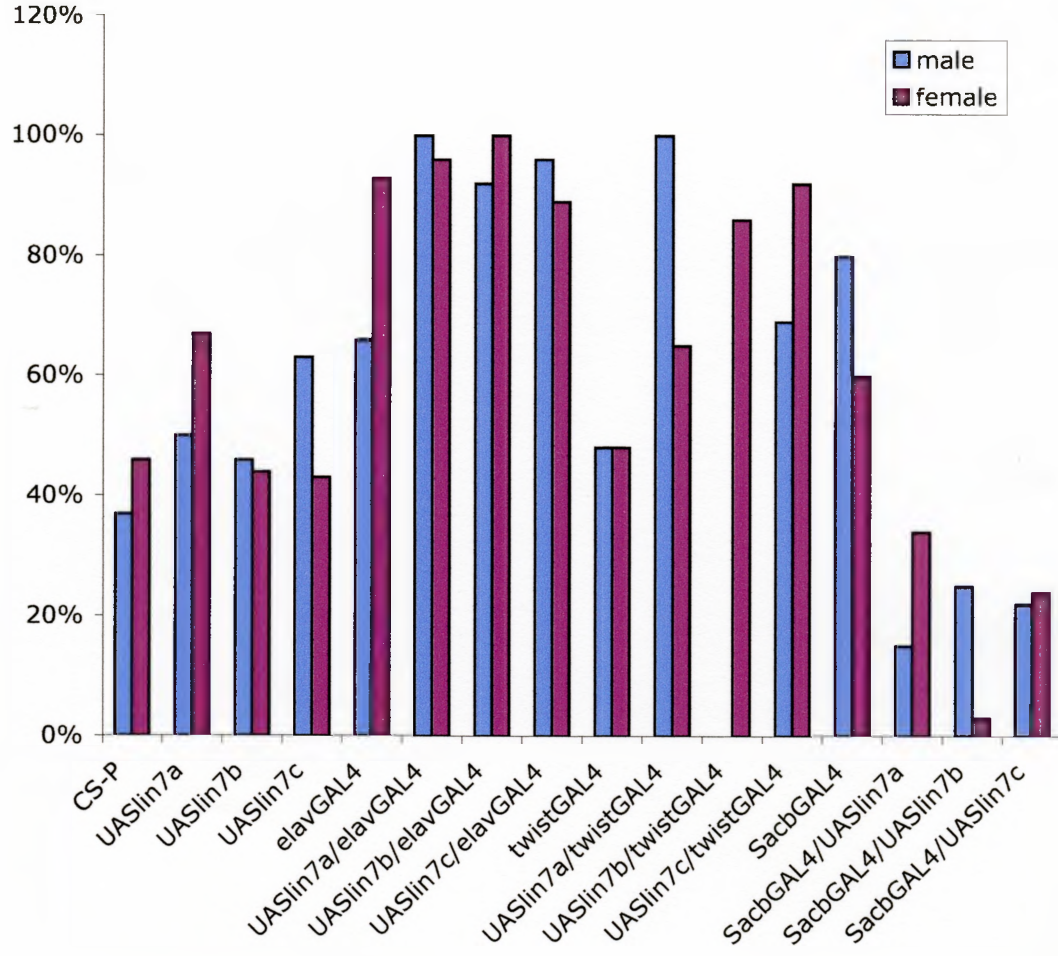
Appendix 1. Adult fly grooming behavior assay

Adult fly grooming behavior test was used to examine the effect of misexpression of *dVELI*. *Drosophila* grooming behavior was described by Dawkins and Dawkins as the leg movement used to clean a certain body part in a fixed pattern. First a leg sweeps a certain body part and then rubs with another leg, usually the contralateral one, to remove the accumulated dust from the sweeping (Dawkins and Dawkins, 1976). Under normal conditions, adult flies show low levels of grooming behavior. However, this behavior can be stimulated when dust is applied. Because this behavior involves the sensory neuron transduction, synaptic connection and muscle function, behavior changes may reflect altered function of genes involved in this neural circuitry (Phillis et al, 1993). Therefore, grooming behavior assay was used in this thesis work to test the potential mutant effects of misexpression of *dveli*.

This grooming behavior assay is adapted from the method used by Phillis et al. to isolate mutants affecting neural circuitry required for grooming behavior in *Drosophila melanogaster* (Phillis et al, 1993). Three to four days old adult flies are dusted with Reactive Yellow 86 (Sigma, #R2879), and then are allowed to clean themselves for 2 hours at room temperature in the “cleaning chamber” (two vials connected at the open ends with holes on the side to allow air flow). After 2 hours, the flies are checked under microscope to see if the ventral part of the body is clean or not. Flies without any yellow dust on the back are recorded as “clean”, flies with yellow dust are recorded as “dusty”. Then the percentage of dusty flies are calculated as dusty flies over total sample number. Because the results of different trials of wild type flies grooming behavior showed a big

range of variation, and potential mutants seem to be cleaner than wild type, this experiment was considered insignificant. The table below shows the pooled data from all the trials. The chart shows the percentage of dusty flies compared between different genotype lines.

2.0mg	male		Total#	% of dusty	female		Total#	% of dusty
	dusty	clean			dusty	clean		
CS-P	32	54	86	37%	40	46	86	46%
UASlin7a	10	10	20	50%	37	18	55	67%
UASlin7b	25	29	54	46%	19	24	43	44%
UASlin7c	31	18	49	63%	21	27	48	43%
elavGAL4	18	9	27	66%	28	2	30	93%
UASlin7a/elavGAL4	28	0	28	100%	27	1	28	96%
UASlin7b/elavGAL4	26	2	28	92%	28	0	28	100%
UASlin7c/elavGAL4	25	1	26	96%	26	3	29	89%
twistGAL4	13	14	27	48%	13	14	27	48%
UASlin7a/twistGAL4	22	0	22	100%	19	10	29	65%
UASlin7b/twistGAL4	0	9	9	0%	26	4	30	86%
UASlin7c/twistGAL4	16	7	23	69%	26	2	28	92%
SacbGAL4	24	6	30	80%	18	12	30	60%
SacbGAL4/UASlin7a	3	17	20	15%	8	15	23	34%
SacbGAL4/UASlin7b	7	20	27	25%	1	26	27	3%
SacbGAL4/UASlin7c	2	7	9	22%	7	22	29	24%



Appendix 2. Time required for adult flies to recover from CO₂ treatment

Flies are put to sleep with CO₂ for 1 minute, after that they are transferred to test tubes (10 flies per tube) for recovery. Time required for 5 flies and 10 flies to awake are recorded. It is hoped that over or misexpression of dVELI might affect the ability of flies to wake up from CO₂ treatment. However, there was a big variation of time required for different groups of the same genotype flies to wake up. Therefore, this experiment was not successful.

Genotype (# of flies pooled from # of tests)	Average time for 5 flies to wake up (min'sec)	Average time for 10 flies to wake up (min'sec)
yw male (80/8)	2'38	5'47
yw female(40/4)	2'05	3'37
elavGAL4 male(40/4)	2'13	4'41
elavGAL4 female(30/3)	2'46	4'05
pGMR GAL4 male(20/2)	1'59	3'52
pGMR GAL4 female (20/2)	1'46	3'00
pGMR GAL4/UASlin-7a female (10/1)	1'35	2'20
pGMR GAL4/UASlin-7a male (20/2)	2'30	3'53
pGMR GAL4/UASlin-7b female (30/3)	1'49	3'01
pGMR GAL4/UASlin-7b male (30/3)	2'42	4'13
pGMR GAL4/UASlin-7c female (20/2)	1'28	2'21
pGMR GAL4/UASlin-7c male (10/1)	1'34	2'15
twist GAL4/UASlin-7a male (48/5)	3'05	4'19
twist GAL4/UASlin-7b male (38/4)	3'43	5'00
twist GAL4/UASlin-7b female (39/4)	2'28	3'12
twist GAL4/UASlin-7c male (50/5)	2'36	4'31
twist GAL4/UASlin-7c female (50/5)	2'05	3'01

Appendix 3. Genetic Scheme for Mapping the Chromosomal Location of UASlin7s

Three UAS lin7 constructs were generated by Allison MacMullin (Jacobs' Lab. McMaster University). The chromosomal locations of the UAS constructs were mapped as showed below. All these lines were crossed to *yw; Sco/CyO; +* females. By the difference shown in the phenotypes of the offspring, the chromosomal locations can be determined.

When located at first chromosome:

$$\begin{array}{c} UAS\ lin7s/Y;+;+ \ X\ yw;Sco/CyO;+ \\ \Downarrow \\ UAS\ lin7s/yw\ or\ yw/Y; \ +/Sco\ or\ +/CyO; \ + \end{array}$$

All males would be white eye and all females would have orange eyes

When located at second chromosome:

$$\begin{array}{c} \text{Step 1 } yw/Y; \ UAS\ lin7s/UAS\ lin7s;+ \ X\ yw;Sco/CyO;+ \\ \Downarrow \\ yw/yw\ or\ yw/Y; \ UAS\ lin7s/Sco\ or\ UAS\ lin7s/CyO;+ \end{array}$$

$$\begin{array}{c} \text{Step 2 } yw/Y; \ UAS\ lin7s/Sco;+ \ X\ yw/yw; \ UAS\ lin7s/CyO;+ \\ \Downarrow \\ yw/Y\ or\ yw/yw; \ UAS\ lin7s/UAS\ lin7s\ or\ UAS\ lin7s/CyO\ or\ UAS\ lin7s/Sco \\ or\ Sco/CyO; \ + \end{array}$$

The possible phenotypes are: orange eyes, orange eyes with missing hair (*Sco*), orange eyes with curly wings (*CyO*) or white eye with both missing hair and curly wings.

When located at third chromosome:

Step 1 $yw/Y; +; UAS\ lin7s/UAS\ lin7s$ X $yw; Sco/CyO; +$
 \downarrow
 yw/yw or $yw/Y; +/Sco$ or $+/CyO; +/UAS\ lin7s$

Step 2 $yw/Y; +/Sco; +/UAS\ lin7s$ X $yw/yw; +/CyO; +/UAS\ lin7s$
 \downarrow
 yw/Y or $yw/yw; ++$ or $+/CyO$ or $+/Sco$ or $Sco/CyO; ++$ or $+/UASlin7s$ or $UASlin7s/UASlin7s$

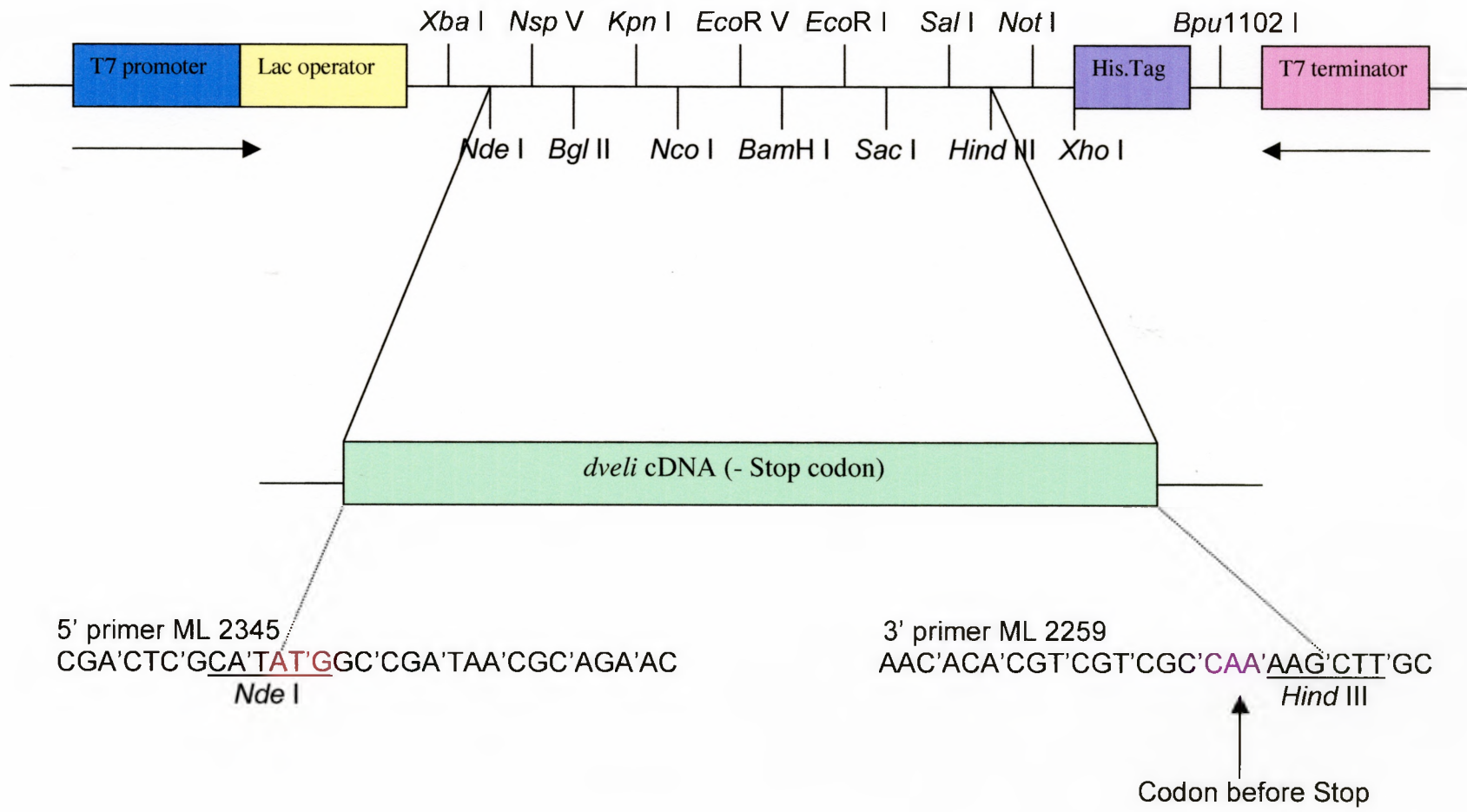
The possible phenotypes are the same four phenotypes that would be observed if the construct is located at second chromosome plus four extra phenotypes: white eyes, white eyes with curly wings, white eyes with missing hair, and orange eyes with both curly wings and missing hair. Therefore, as long as the white eye only flies are observed, the location of the UAS construct is mapped to be on the third chromosome.

All three UAS *lin7* constructs are on third chromosome according to this mapping scheme.

Appendix 4. pET29b+ multiple cloning sites

This figure shows the multiple cloning sites of pET29b+ vector (Novagen) and the insertion site of *dveli* for making the dVELI-His fusion protein construct. The primers used for amplifying *dveli* cDNA are shown in the figure, both primer sequences shown in the figure are in 5' to 3' direction using the coding strand of the cDNA sequence.

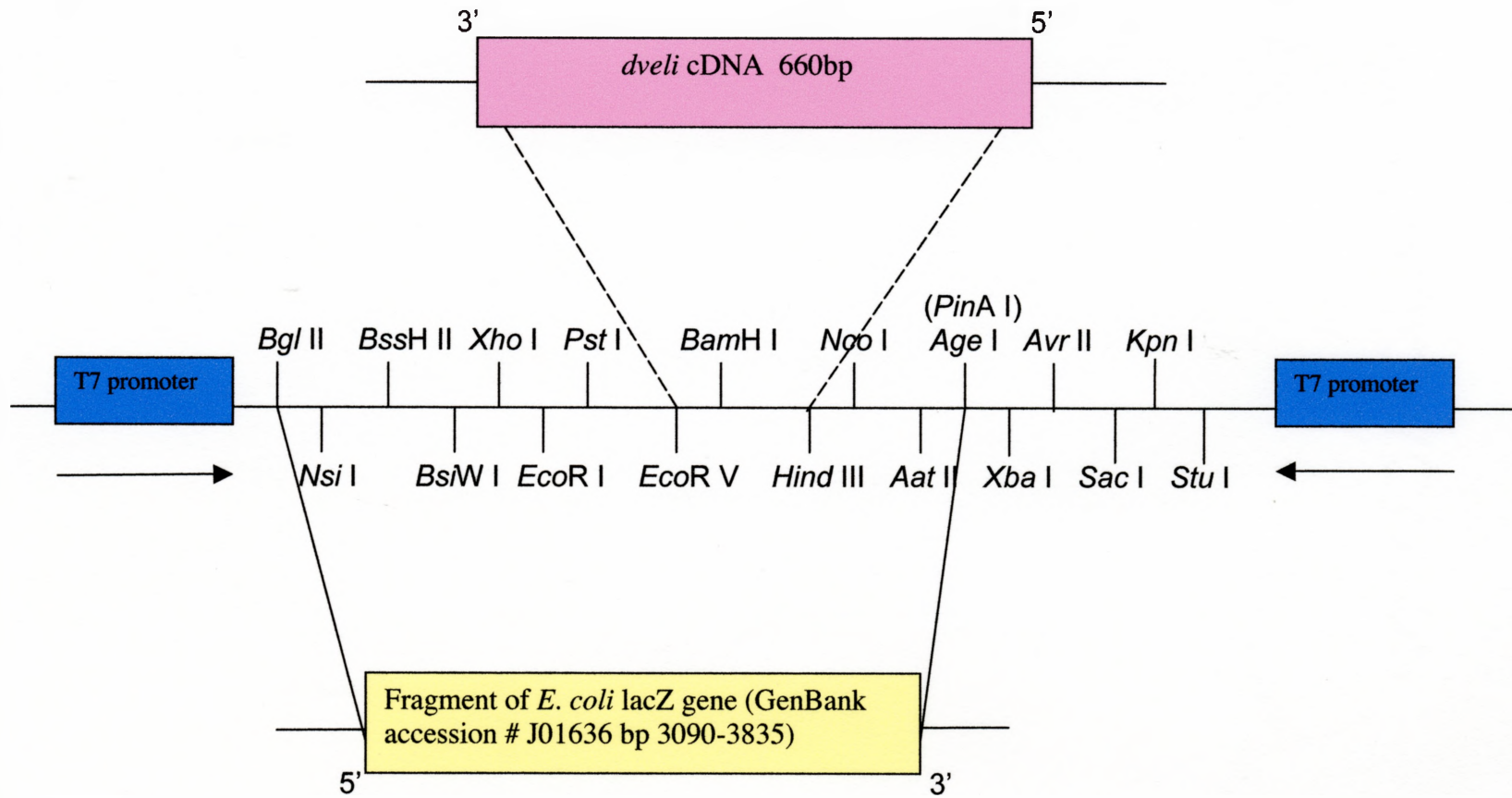
pET-29b(+) multiple cloning sites



Appendix 5. LITMUS 28i multiple cloning sites

The figure shows the multiple cloning sites of LITMUS 28i vector (New England Biolabs). The insert sites of both *dveli* and *lacZ* are shown in the figure. There are two T7 promoters in opposite directions flanking the multiple cloning sites. They are used for the transcription of two complementary RNA strands, which are then annealed to each other to produce the double-stranded RNA.

LITMUS 28i multiple cloning sites

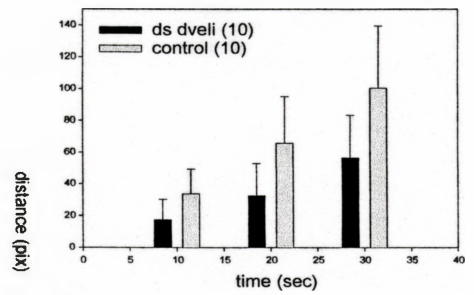


Appendix 6. Locomotion behavior test of dsRNA treated larvae

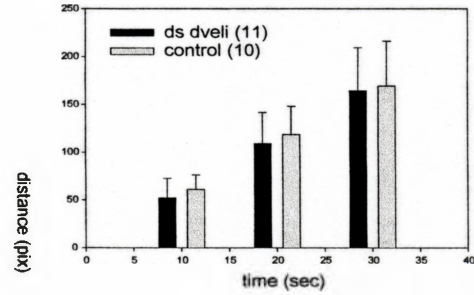
Behavior tests were done as described in methods and results. The charts shown here are the results of several trials. Test 1 was using younger larvae (~86 hours old) fed with lower dosage of dsRNA (400ng/ μ l). The result shows that larvae fed with *ds dveli* move slower than the control. However, the variation among the larvae is very large (shown by the error bar), therefore, the result is insignificant. Tests 2 and 3 used larvae fed at the same time but tested at different ages (92-hour-old and 110-hour-old, respectively). The results show that the moving speed difference between the *ds dveli* and control larvae is more noticeable when the larvae are older. Still the variation among the tested animal is large, therefore, the results are inconclusive. Tests 4 and 5 show that when more dsRNA were fed to the larvae (900ng/ μ l), the results are more significant as the variation become smaller. Also, in test 5 a negative control was added (*ds lacZ*) showing that the slower locomotion behavior is not likely due to any dsRNA treatment but more likely as a specific interference of *dveli* function by double-stranded *dveli* RNA. Tests 6 and 7 show results of larvae fed at the same time but tested at different ages (107 and 131-hour-old, respectively). Again, the results show that larvae fed with *ds dveli* move slower than the control ones (without ds RNA or with *ds lacZ* feeding). However, because of the small sample size, the result is insignificant. Tests 8 and 9 are repeating tests with 108 hours old and 114 hours old larvae, respectively.

Although there are variations among these tests, the general pattern is that larvae treated with *ds dveli* move slower than control ones.

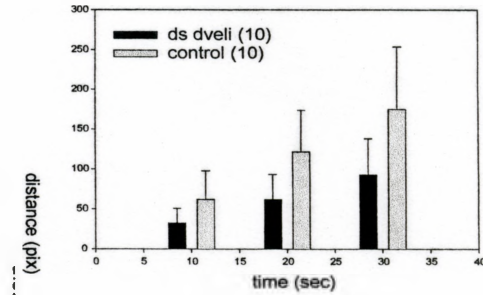
Test 1-400ng/ul, 86hr



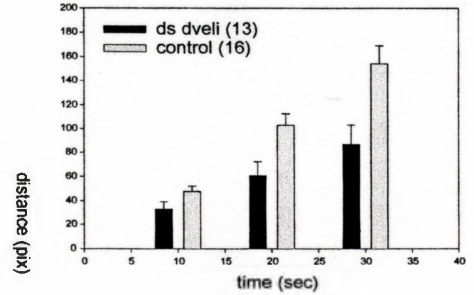
Test 2-400ng/ul, 92 hr



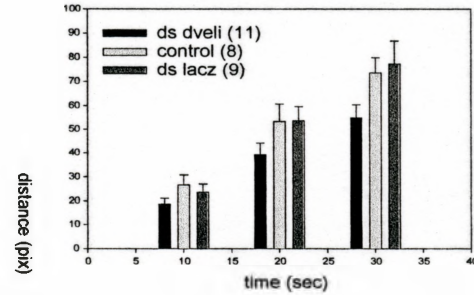
Test 3-400ng/ul, 110 hr



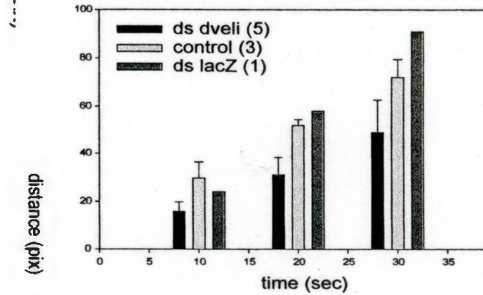
Test 4-900ng/ul, 110 hr



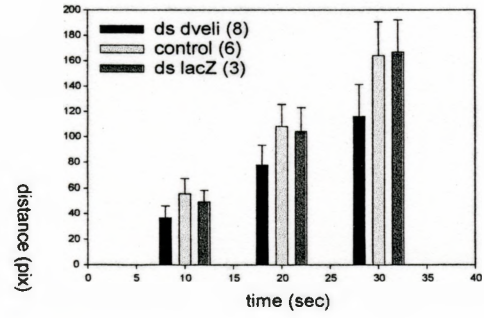
Test 5-900ng/ul, 110hr



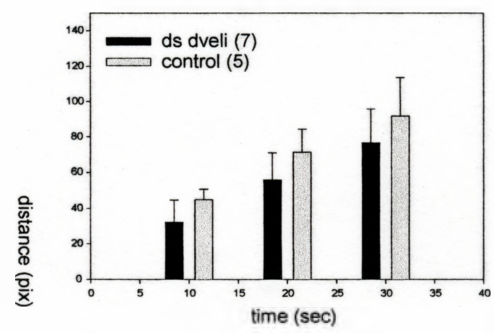
Test 6-900ng/ul, 107hr



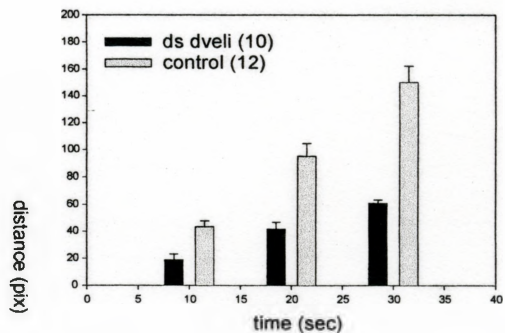
Test 7-900ng/ul, 131hr



Test 8-900ng/ul, 108hr



Test 9-900ng/ul, 114hr

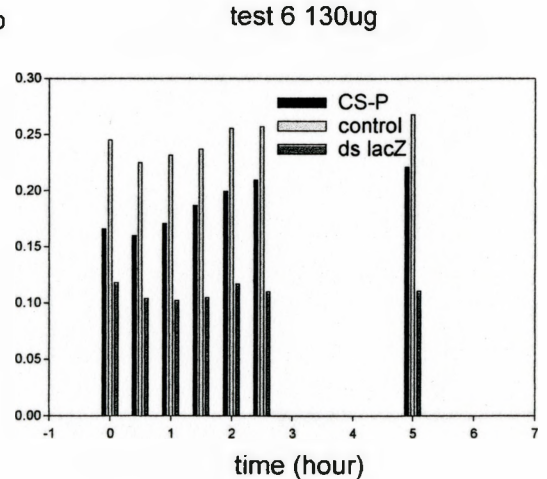
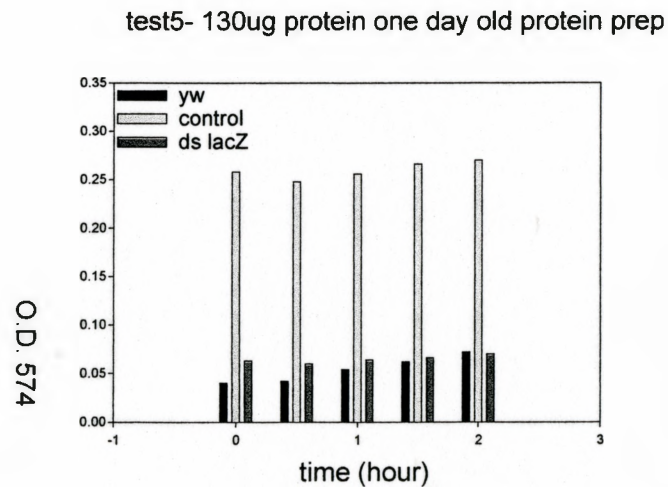
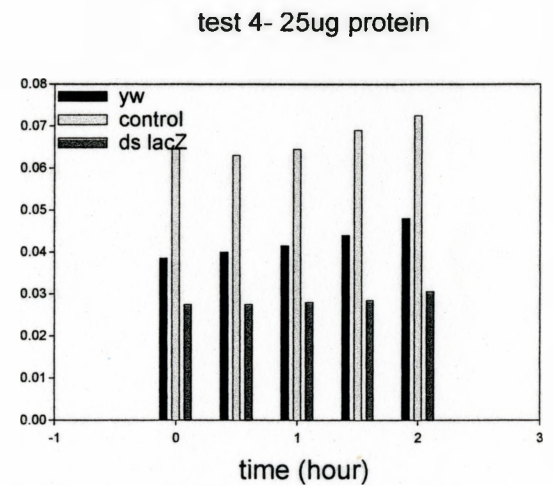
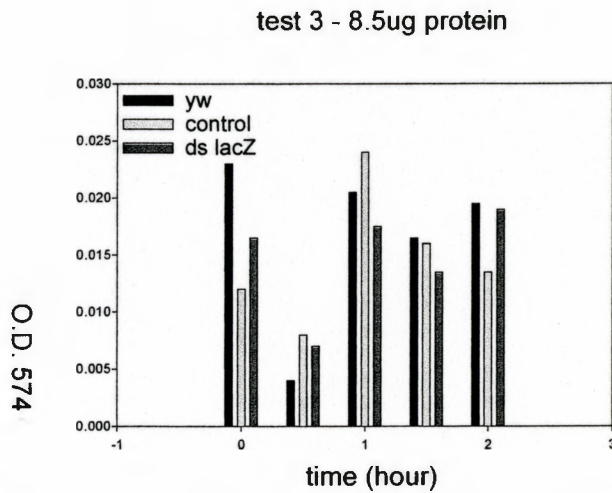
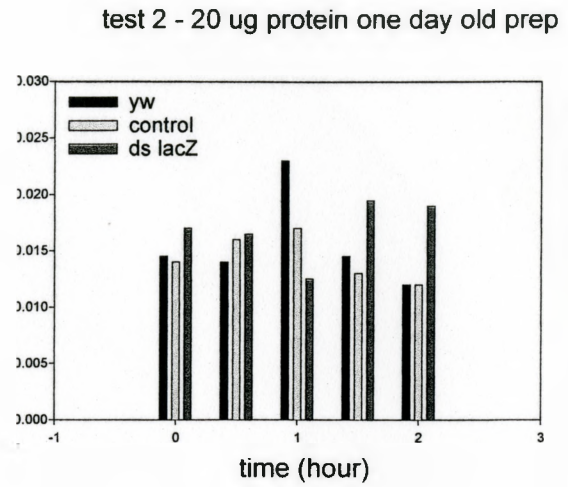
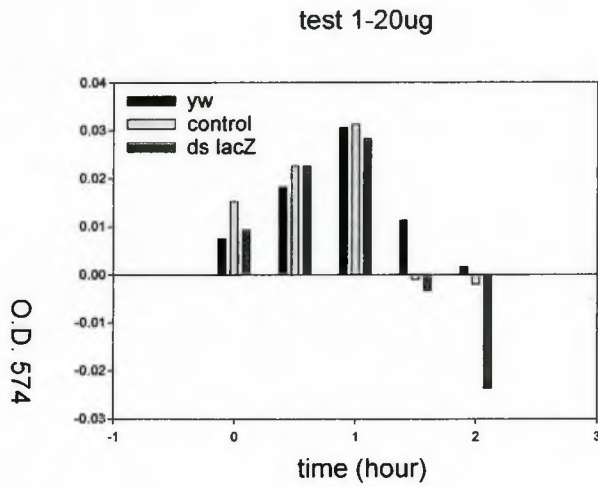


Appendix 7. β -galactosidase activity assay for *ds lacZ* efficiency

A *ds lacZ* construct was made as described in Methods. The reason of making this construct is to use the double-stranded *lacZ* RNA as a negative control for the RNAi experiments. To make sure this construct is working, β -galactosidase activity was tested using the fly line that contain a *lacZ* reporter, *Slit 1.0 lacZ*. Late stage embryos of *Slit 1.0 lacZ* flies were either soaked in double-stranded *lacZ* RNA (*ds lacZ*) solution or in RNAi solution (control) without any RNA. Third instar larvae from this treatment were later used for quantitative β -galactosidase activity assay following the protocol from *Drosophila* protocol book and method used by Yamaguchi et al. (Yamaguchi et al, 1997). This method uses the β -galactosidase substrate chlorophenol red β -D-galactopyranoside (CPRG) as an indication of β -galactosidase activity. CPRG is a galactoside analog which is hydrolyzed by the enzyme β -galactosidase. When CPRG is hydrolyzed, it breaks down into galactose and chlorophenol red, which is a water-soluble red substrate that turns the solution from yellow to red color. The color change intensities can be detected by spectrophotometer.

Protein extract from the dsRNA treated larvae (*ds lacZ*), control and *yw*⁻ larvae were tested with the CPRG containing solution. *yw*⁻ was used as endogenous β -galactosidase activity control (Yamaguchi et al, 1997). If the *ds lacZ* construct worked, the β -galactosidase activity should be lower in the larvae that were fed with *ds lacZ*. Several tests were done as shown in the figure. There were variations, therefore, the results of this assay is inconclusive. Although the test 4 did show lower β -galactosidase activity in *ds lacZ* larvae, the difference in the absorbance reading is very small, thus the difference

is insignificant. Tests 5 and 6 showed a larger difference between the control and *ds lacZ*, however, large amount of protein extracts were added compared to the first four tests. Although the same amount of protein extracts were used in these two trials, the activities of wild type control and *ds lacZ* fed larvae showed variations. Also, the activities levels didn't change over the incubation time period (2 hours), which indicated problems with either the *lacZ* expression or enzyme activity.



Appendix 8. Deficiency screen results

The results of the deficiency screen for all the 107 homozygously lethal lines are summarized in the table below. The expected phenotypes ratio for the lines that have lethal insertions in the deficiency region (96A17-21 to 96D1) is normal body color, non-*Sb*: normal body color, *Sb*: dark body color, *Sb* = 1:1:1. Otherwise the ratio should be 2:1:1.

From this screen, 21 of them are most likely to have lethal insertions in the deficiency regions since they show ratios that are close to the expected 1:1:1 value. These lines are indicated in bold letters. 48 lines show results that are close to the 2:1:1 ratio for insertions that lie outside of the deficiency. However, the accuracy of this screen is questionable since the rest of them show ratio values that are not even close to either one of the expected values (showed in italic letters). It might be because that the deletion over the balancer and the duplication over the balancer genotypes flies are weaker as showed in the control cross (please refer to figure 6), and different P element insertions may have different viability levels.

P element within deficiency (ratio close to 1:1:1)		P element outside of deficiency (ratios close to 2:1:1)				Uncharacterized (ratios not close to either estimated ones)	
N31	1.3:1.2:1(136)	Q37	2.2:1:1.3(222)	N10	1.8:1:1.2(408)	E22	4.6:1:2.8(195)
P71	1.2:1:1(218)	P1	2.1:1:1(172)	P5	2.1:1.2:1(305)	E15	2.5:1:1(166)
O24	1.4:1:1(295)	O55	2.1:1:1.2(276)	O27	1.9:1:1(166)	E33	1.5:1:1:1(203)
P2	1.2:1:1(210)	O70	2:1:1(233)	F12	1.7:1.1:1(159)	J12	1.6:1:1.2(257)
O3	1.4:1:1(182)	O35	2.1:1:1(132)	N23	2.5:1:1.4(298)	S30	3.3:1:1.1(258)
Q31	1.4:1:1(241)	N45	2.2:1:1.3(218)	P68	2.4:1.2:1(200)	I16	5.8:1:2.5(141)
P6	1.3:1:1.1(277)	O72	2:1:1(131)	O17	1.8:1:1(209)	N1	2.5:1:1.5(142)
P57	1.4:1:1(169)	J39	2:1:1.4(184)	K49	2.1:1:1.1(200)	G1	2.9:1:1.1(201)
Q65	1.3:1:1(210)	K28	2.1:1:1.5(189)	J33	1.8:1:1.1(166)	K50	3.9:3:1(296)
K72	1.5:1:1(202)	J46	2:1:1(196)	P56	1.7:1:1(177)	K43	3.1:1:1.6(122)
E29	1.4:1:1.2(189)	N9	2.1:1:1.1(123)	R7	1.9:1:1.2(192)	O26	2.9:1:1.5(272)
C62	1.5:1:1.4(164)	I34	1.6:1:1(209)	F2	2.2:1.5:1(161)	I8	2.7:1:1.5(185)
H32	1.4:1:1(309)	G18	2.2:1:1.5(214)	K44	2.3:1:1.2(304)	Q62	2.3:1:1.5(155)
G57	1.4:1:1.1(255)	G13	2.3:1:1(234)	K40	2.3:1:1.3(172)	N56	1.9:1:1.6(119)
H26	1.3:1:1.1(178)	H56	2.3:1:1.3(225)	K12	2.1:1:1.3(189)	I6	1.8:1.4:1(268)
P10	1.3:1:1.1(298)	F1	2:1.2:1(241)	G9	2.5:1:1.3(158)	K25	3.1:1:1(149)
N62	1.3:1:1.1(236)	K32	2.3:1.4:1(216)	Q35	1.6:1.1:1(145)	Q46	1.8:1:1.4(209)
P19	1.3:1:1.1(272)	D10	2:1:1(225)	O48	2.2:1.4:1(302)	G30	3:1:1.8(188)
N64	1.5:1:1(157)	C19	1.7:1.1:1(187)	R12	1.9:1:1(179)	J18	2.6:1:1.6(207)
O50	1.3:1:1.1(325)	D11	2.3:1:1.5(202)	I1	2.3:1:1.4(246)	G25	2.5:1:1.7(217)
N59	1.4:1:1(144)	Q32	1.9:1:1(202)	N22	1.8:1:1(169)	G55	2.6:1.6:1(173)
		I7	1.8:1:1.3(206)	E32	1.9:1:1(269)	N12	2.6:1:1.6(153)
		N19	2.2:1:1.4(255)	E30	2.2:1.1:1(163)	Q19	2.1:1:1.6(220)
		O62	1.9:1:1.4(199)	Q24	1.8:1:1.3(164)	R3	2.8:1:1.1(79)
		N60	2:1.4:1(214)			Q33	2.5:1:1.8(205)
						O46	3.1:1:1.1(138)
						P69	2.9:1.5:1(214)
						O47	3.1:1:2.3(149)
						H37	2.9:1:1.6(208)
						I9	2.6:1:1.4(268)
						L16	2.1:1:1.6(276)
						O16	2.3:1:1.6(283)
						O28	2.9:1:1.7(171)
						N35	3.4:1:1.6(134)
						N51	1.8:1.7:1(147)
						O61	2.3:1:1.6(262)
						O22	2:1:1.8(140)